CHAPTER 13: REACTIONS AT THE EARTH'S SURFACE: WEATHERING, SOILS, AND STREAM CHEMISTRY

INTRODUCTION

The geochemistry of the Earth's surface is dominated by aqueous solutions and their interactions with rock. We saw in the last chapter that the upper continental crust has the approximate average composition of granodiorite, and that the oceanic crust consists of basalt. But a random sample of rock from the crust is unlikely to be either; indeed it many not be an igneous rock at all. At the very surface of the Earth, sediments and soils predominate. Both are ultimately produced by the interaction of water with "crystalline rock" (by which we mean igneous and metamorphic rocks). Clearly, to fully understand the evolution of the Earth, we need to understand the role of geochemical processes involving water.

Beyond that, water is essential to life and central to human activity. We use water for drinking, cooking, agriculture, heating, cooling, resource recovery, industrial processing, waste disposal, transportation, fisheries, etc. Water chemistry, i.e., the nature of solutes dissolved in it, is the primary factor in the suitability of water for human use. "Polluted" water is unsuitable for drinking and cooking; saline water is unsuitable for these uses as well as agriculture and many industrial uses, etc. We have been particularly concerned with water pollution in the past few decades; that is with the impact of human activity on water chemistry. Both our advancing technology and our exponentially increasing numbers have made pollution problems progressively worse, particularly over the past century. However, we have also become more aware of the adverse impact of poor water quality on human health and the quality of life, and perhaps less tolerant of it as well.

Understanding and addressing problems of water pollution requires an understanding of the behavior of natural aqueous systems for at least two reasons. First, to identify pollution, we need to know the characteristics of natural systems. For example, Pb can be highly toxic, and high concentrations of Pb in the blood have been associated with learning disabilities and other serious problems. However, essentially all waters have some finite concentration of Pb; we should be concerned only when Pb concentrations exceed natural levels. Second, natural processes affect pollutants in the same way they affect their natural counterparts. For example, cadmium leached from landfills will be subject to the same adsorption/desorption reactions as natural Cd. To predict the fate of pollutants, we need to understand those processes.

In this chapter, we focus on water and its interaction with solids at the Earth's surface. We can broadly distinguish two kinds of aqueous solutions: continental waters and seawater. Continental waters by this definition include ground water, fresh surface waters (river, stream and lake waters), and saline lake waters. The compositions of these fluids are obviously quite diverse. Seawater, on the other hand, is reasonably uniform, and it is by far the dominant fluid on the earth's surface. Hydrothermal fluids are third class of water produced when water is heated and undergoes accelerated interactions with rock and often carry a much higher concentration of dissolved constituents than fresh water. Our focus in this chapter will be on the chemistry of continental waters and how they interact with rock. We we consider seawater in Chapter 15.

REDOX IN NATURAL WATERS

The surface of the Earth represents a boundary between regions of very different redox state. The atmosphere contains free oxygen and therefore is highly oxidizing. In the Earth's interior, however, there is no free oxygen, Fe is almost entirely in the 2+ valance state, reduced species such as CH_4, CO, and S_2 exist, and conditions are quite reducing. Natural waters exist in this boundary region and their redox state, perhaps not surprisingly, is highly variable. Biological activity is the principal cause of this variability. Plants (autotrophs) use solar energy to drive thermodynamically unfavorable

photosynthetic reactions that produce free O_2, the ultimate oxidant, on the one hand and organic matter, the ultimate reductant, on the other. Indeed it is photosynthesis that is responsible for the oxidizing nature of the atmosphere and the redox imbalance between the Earth's exterior and interior. Both plants and animals (heterotrophs) liberate stored chemical energy by catalyzing the oxidation of organic matter in a process called *respiration*. The redox state of solutions and solids at the Earth's surface is largely governed by the balance between photosynthesis and respiration. By this we mean that most waters are in a fairly oxidized state because of photosynthesis and exchange with the atmosphere. When they become reducing, it is most often because respiration exceeds photosynthesis and they have been isolated from the atmosphere. Water may also become reducing as a result of reaction with sediments deposited in ancient reduced environments, but the reducing nature of those ancient environments resulted from biological activity. Weathering of reduced primary igneous rocks also consumes oxygen, and this process governs the redox state of some systems, mid-ocean ridge hydrothermal solutions for example. On a global scale, however, these processes are of secondary importance for the redox state of natural waters.

The predominant participants in redox cycles are C, O, N, S, Fe, and Mn. There are a number of other elements, for example, Cr, V, As, and Ce, that have variable redox states; these elements, however, are always present in trace quantities and their valance states reflect, rather than control, the redox state of the system. Although phosphorus has only one valance state (+V) under natural conditions, its concentration in solution is closely linked to redox state because the biological reactions that control redox state also control phosphorus concentration, and because it is so readily adsorbed on Fe oxide surfaces.

Water in equilibrium with atmospheric oxygen has a pε of +13.6 (at pH = 7). At this pε, thermodynamics tells us that all carbon should be present as CO_2 (or related carbonate species), all nitrogen as NO_3^-, all S as $SO_4^=$, all Fe as Fe^{3+}, and all Mn as Mn^{4+}. This is clearly not the case and this disequilibrium reflects the kinetic sluggishness of many, though not all, redox reactions[£]. Given the disequilibrium we observe, the applicability of thermodynamics to redox systems would appear to be limited. Thermodynamics may nevertheless be used to develop partial equilibrium models. In such models, we can make use of *redox couples* that might reasonably be at equilibrium to describe the redox state of the system. In Chapter 3, we introduced the tools needed to deal with redox reactions: E_H, the hydrogen scale potential (the potential developed in a standard hydrogen electrode cell) and pε, or electron activity. We found that both may in turn be related to the Gibbs Free Energy of reaction through

TABLE 13.1. pε VALUES OF PRINCIPLE AQUATIC REDOX COUPLES

	Reaction	pε°	$pε_W$
1	$\frac{1}{4}O_{2(g)} + H^+ + e^- \rightleftarrows \frac{1}{2}H_2O$	+20.75	+13.75
2	$\frac{1}{5}NO_3^- + \frac{6}{5}H^+ + e^- \rightleftarrows \frac{1}{10}N_{2(g)} + \frac{3}{5}H_2O$	+21.05	+12.65
3	$\frac{1}{2}MnO_{2(s)} + 2H^+ + e^- \rightleftarrows \frac{1}{2}Mn^{2+} + H_2O$	+20.8	+9.8†
4	$\frac{5}{4}NO_3^- + \frac{6}{5}H^+ + e^- \rightleftarrows \frac{1}{8}NH_4^+ + \frac{3}{8}H_2O$	+14.9	+6.15
5	$Fe(OH)_{3(s)} + 3H^+ + e^- \rightleftarrows Fe^{2+} + 3H_2O$	+16.0	+1.0†
6	$\frac{1}{2}CH_2O^* + H^+ + e^- \rightleftarrows \frac{1}{2}CH_3OH$	+4.01	-3.01
7	$\frac{1}{8}SO_4^{2-} + \frac{5}{4}H^+ + e^- \rightleftarrows \frac{1}{8}H_2S + \frac{1}{2}H_2O$	+5.25	-3.5
8	$\frac{1}{8}SO_4^{2-} + \frac{9}{8}H^+ + e^- \rightleftarrows \frac{1}{8}HS^- + \frac{1}{2}H_2O$	+4.25	-3.6
9	$\frac{1}{8}CO_{2(g)} + H^+ + e^- \rightleftarrows \frac{1}{8}CH_{4(g)} + \frac{1}{4}H_2O$	+2.9	-4.1
10	$\frac{1}{6}N_{2(g)} + \frac{4}{3}H^+ + e^- \rightleftarrows \frac{1}{3}NH_4^+$	+4.65	-4.7
11	$\frac{1}{4}CO_{2(g)} + H^+ + e^- \rightleftarrows \frac{1}{4}CH_2O^* + \frac{1}{4}H_2O$	-0.2	-7.2

† The concentration of Mn^{2+} and Fe^{2+} are set to 1 μM.
* We are using "CH_2O", which is formally formaldahyde, as an abbreviation for organic matter generally (for example, glucose is $C_6H_{12}O_6$).

£ While this may make life difficult for geochemists, it is also what makes it possible in the first place. We, like all other organisms, consist of a collection of reduced organic species that manage to persist in an oxidizing environment!

the Nernst Equation (equ. 3.121). These are all the tools we need; in this section, we will see how we can apply them to understanding redox in aqueous systems.

Table 13.1 lists the pε° of the most important redox half reactions in aqueous systems. Also listed are $p\varepsilon_W$ values. $p\varepsilon_W$ is the pε° when the concentration of H^+ is set to 10^{-7} (pH = 7). The relation between pε° and $p\varepsilon_W$ is simply:

$$p\varepsilon_W = p\varepsilon^\circ + \log [H^+]^\nu = p\varepsilon^\circ - \nu \times 7$$

Reactions are ordered by decreasing $p\varepsilon_W$ from strong oxidants at the top to strong reductants at the bottom. In this order, each reactant can oxidize any product below it in the list, but not above it. Thus sulfate can oxidize methane to CO_2, but not ferrous iron to ferric iron. Redox reactions in aqueous systems are often biologically mediated. In the following section, we briefly explore the role of the biota in controlling the redox state of aqueous systems.

Biogeochemical Redox Reactions

As we noted above, photosynthesis and atmospheric exchange maintains a high pε in surface waters. Water does not transmit light well, so there is an exponential decrease in light intensity with depth. As a result, photosynthesis is not possible below depths of 200 m even in the clearest waters. In murky waters, photosynthesis can be restricted to the upper few meters or less. Below this "photic zone", biologic activity and respiration continue, sustained by falling organic matter from the photic zone. In the deep waters of lakes and seas where the rate of respiration exceeds downward advection of oxygenated surface water, respiration will consume all available oxygen. Once oxygen is consumed, a variety of specialized bacteria continue to consume organic matter and respire utilizing oxidants other than oxygen. Thus pε will continue to decrease.

Since bateria exploit first the most energetically favorable reactions, Table 13.1 provides a guide the sequence in which oxidants are consumed as pε decreases. From it, we can infer that once all molecular oxygen is consumed, reduction of nitrate to molecular nitrogen will occur (reaction 2). This processes, known as *denitrification*, is carried out by bacteria, which use the oxygen liberated to oxidize organic matter and the net energy liberated to sustain themselves. At lower levels of pε, other bacteria reduce nitrate to ammonia (reaction 4), a process called *nitrate reduction*, again using the oxygen liberated to oxidize organic matter. At about this pε level, Mn^{4+} will be reduced to Mn^{2+}. At lower pε, ferric iron is reduced to ferrous iron. The reduction of both Mn and Fe may also be biologically mediated in whole or in part.

From Table 13.1, we can expect that *fermentation* (reaction 6 in Table 13.1) will follow reduction of Fe. Fermentation can involve any of a number of reactions, only one of which, reduction of organic matter (carbohydrate) to methanol, is represented in Table 13.1. In fermentation reactions, further reduction of some of the organic carbon provides a sink of electrons, allowing oxidation of the remaining organic carbon; for example in glucose, which has 6 carbons, some are oxidized to CO_2 while others are reduced to alcohol or acetic acid. While these kinds of reactions can be carried out by many organisms, it is bacterial-me-

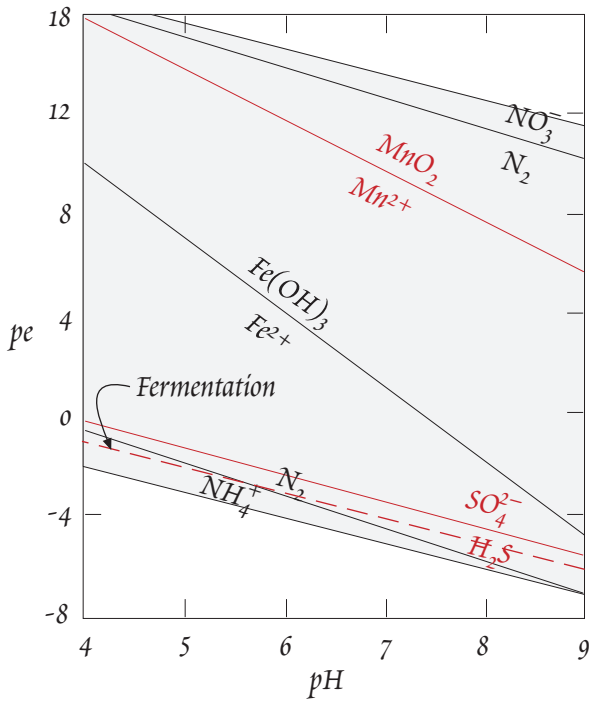

Figure 13.1. Important biogeochemical redox couples in natural waters.

diated fermenation that is of geochemical interest.

At lower pε, sulfate is used as the oxidant by sulfate-reducing bacteria to oxidize organic matter, and at even lower pε, nitrogen is reduced to ammonia (reaction 9), a process known as *nitrogen fixation*, with the nitrogen serving an the electron acceptor for the oxidization of organic matter. This reaction is of great biological importance, as nitrogen is an essential ingredient of key biological compounds such as proteins and DNA (see Chapter 14), and hence is essential to life; all plants must therefore take up inorganic nitrogen. While a few plants, blue-green algae (cyanobacteria) and legumes, can utilize N_2, most require "fixed" nitrogen (ammonium, nitrate, or nitrite). Hence nitrogen-fixing bacteria play an essential role in sustaining life on the planet.

To summarize, in a water, soil, or sediment column where downward flux of oxygen is less than the downward flux of organic matter, we would expect to see oxygen consumed first, followed by reduction of nitrate, manganese, iron, sulfur, and finally nitrogen. This sequence is illustrated on a pε-pH diagram in Figure 13.1. We would expect to see a similar sequence with depth in a column of sediment where the supply of organic matter exceeds the supply of oxygen and other oxidants.

EUTROPHICATION

The extent to which the redox sequence described above proceeds in a body of water depends on a several factors. The first of these is temperature structure, because this governs the advection of oxygen to deep waters. As mentioned above, light (and other forms of electromagnetic energy) is not transmitted well by water. Thus only surface waters are heated by the Sun. As the temperature of surface water rises, its density decreases (fresh water reaches it greatest density at 4° C). These warmer surface waters, known in lakes as the *epilimnion*, generally overlie a zone where temperature decreases rapidly, known as the *thermocline* or *metalimnion*, and a deeper zone of cooler water, known as the *hypolimnion*. This temperature stratification produces a stable density stratification which prohibits vertical advection of water and dissolved constitutents, including oxygen and nutrients. In tropical lakes and seas, this stratification is permanent. In temperate regions, however, there is an annual cycle in which stratification develops in the spring and summer. As the surface water cools in the fall and winter, its density decreases below that of the deep water and vertical mixing occurs. The second important factor governing the extent to which reduction in deep water occurs is nutrient levels. Nutrient levels limit the amount of production of organic carbon by photosynthesizers (in lakes, phosphorus concentrations are usually limiting; in the oceans, nitrate and micronutrients such as iron appear to be limiting). The availability of organic carbon in turn controls *biological oxygen demand* (BOD) In water with high nutrient levels there is a high flux of organic carbon to deep waters and hence higher BOD.

In lakes with high nutrient levels, the temperature stratification described above can lead to a situation where dissolved oxygen is present in the epilimnion and absent in the hypolimnion. Regions where dissolved oxygen is present are termed *oxic*, those where sulfide or methane are present are called *anoxic*. Regions of intermediate pε are called *suboxic*. Lakes are where suboxic or anoxic conditions exist as a result of high biological producitivy are said to be *eutrophic*. This occurs naturally in many bodies of water, particularly in the tropics where stratification is permanent. It can also occur, however, as a direct result addition of pollutants such as sewage to the water, and an indirect result of pollutants such as phosphate and nitrate. Addition of the latter enhances productivity and availability of organic carbon, and ultimately BOD. When all oxygen is consumed conditions become anaerobic and the body of water becomes eutrophic. Where this occurs naturally, ecosystems have adapted to this circumstance and only anaerobic bacteria are found in the hyperlimnion. When it results from pollution, it can be catastrophic for macrofauna such as fish that cannot tolerate anaerobic conditions.

Chapter 13: Weathering, Soils, and Stream Chemistry

Redox and Biological Primary Production

The biota is capable of oxidations as well as reductions. The most familiar of these reactions is photosynthesis. Most organisms capable of photosynthesis, which includes both higher plants and a variety of single-celled organisms, produce oxygen as a biproduct of photosynthesis:

$$CO_2 + H_2O \rightleftarrows CH_2O + O_2 \qquad 13.1$$

However, there are also photosynthesis pathways that do not produce O_2. Green and purple sulfur bacteria are phototrophs that oxidize sulfide to sulfur in the course of photosynthesis:

$$CO_2 + 2H_2S \rightleftarrows CH_2O + \tfrac{1}{4}S_8 + H_2O \qquad 13.2$$

This reaction requires considerably less light energy (77.6 vs. 476 kJ/mol) than oxygenic photosynthesis, enabling these bacteria survive at lower light levels than green plants.

While photosynthesisis is far and away the primary way in which organic carbon is produced or "fixed", chemical energy rather than light energy may also be used to fix organic carbon in processes collectively known as *chemosynthesis*. In chemosynthesis, the energy liberated in oxidizing reduced inorganic species is used to reduce CO_2 to organic carbon. For example, nitrifying bacteria oxidize ammonium to nitrite in a process known as *nitrification*:

$$CO_2 + \tfrac{2}{3}NH_4 + \tfrac{1}{3}H_2O \rightleftarrows CH_2O + \tfrac{2}{3}NO_2^- + \tfrac{4}{3}H^+ \qquad 13.3$$

Colorless sulfur bacteria oxidize sulfide to sulfate in fixing organic carbon:

$$CO_2 + H_2S + O_2 + H_2O \rightleftarrows CH_2O + SO_4^{2-} + 2H^+ \qquad 13.4$$

Redox Buffers and Transition Metal Chemistry

The behavior of transition metals in aqueous solutions and solids in equilibrium with them is particularly dependent on redox state. Many transition metals have more than one valence state within the range of pε of water. In a number of cases, the metal is much more soluble in one valence state than in others. The best examples of this behavior are provided by iron and manganese, both of which are much more soluble in their reduced (Fe^{2+}, Mn^{2+}) than in oxidized (Fe^{3+}, Mn^{4+}) forms. Redox conditions thus influence a strong control on the concentrations of these elements in natural waters.

Because of the low solubility of their oxidized formes, the concentrations of Fe, Mn, and similar metals are quite low under "normal" conditions, i.e., high pε and near-neutral pH. There two common circumstances where higher Fe and Mn concentrations in water occur. The first is when sulfide ores are exposed by mining and oxidized to sulfate, e.g.:

$$2FeS_{2(s)} + 2H_2O + 7O_2 \rightleftarrows 4H^+ + 4SO_4^{2-} + 2Fe^{2+}$$

This can dramatically lower the pH of streams draining such areas. The lower pH in turn allows higher concentrations of dissolved metals (e.g., Figure 13.2), even under oxidizing conditions. The second circumstance where higher Fe and Mn concentrations occur is under suboxic or anoxic conditions that may occur in deep waters of lakes and seas as well as sediment pore waters. Under these circumstances Fe and Mn are

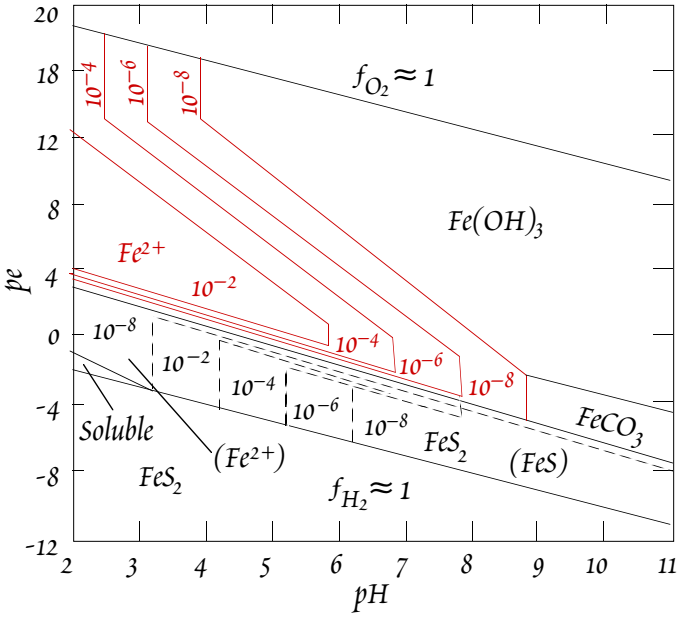

Figure 13.2. Contours of dissolved Fe activity as a function of pε and pH.

reduced to their soluble forms, allowing much higher concentrations.

In cases where precipitation or solution involves a change in valence or oxidation state, the solubility product must include pε or some other redox couple, e.g.:

$$Fe_2O_3 + 6H^+ + 2e^- \rightleftarrows 2Fe^{2+} + 3H_2O \qquad K = \frac{a^2_{Fe^{2+}}}{a^6_{H^+} a^2_{e^-}} \qquad 13.5$$

In Chapter 3, we noted that pε is often difficult to determine. One approach to the problem is to assume the redox state in the solution is controlled by a specific reaction. The controlling redox reactions will be those involving the most abundant species; very often this is sulfate reduction:

$$\frac{1}{8}SO_4^{2-} + \frac{5}{4}H^+ + e^- \rightleftarrows \frac{1}{8}H_2S + \frac{1}{2}H_2O \qquad 13.6$$

in which case pε is given by:

$$p\varepsilon = p\varepsilon^\circ - \frac{1}{8}\ln\frac{[H_2S]}{[SO_4^{2-}]} - \frac{4}{5}pH \qquad 13.7$$

Under the assumption that this reaction controls the redox state of the solution, electrons may be eliminated from other redox reactions by substituting the above expression. For example, iron redox equilibrium may be written as:

$$\frac{1}{8}SO_4^{2-} + \frac{5}{4}H^+ + Fe^{2+} \rightleftarrows \frac{1}{8}H_2S + \frac{1}{2}H_2O + Fe^{3+} \qquad 13.8$$

In this sense, the pε of most natural waters will be controlled by a *redox buffer*, a concept we considered in Chapter 3. Example 13.1 illustrates this approach.

Example 13.1. Redox State of Lake Water

Consider water of the hypolimnion of a lake in which all oxygen has been consumed and with the following initial composition: $SO_4 = 2 \times 10^{-4}$ M, $\Sigma Fe^{3+} = 10^{-6}$ M, Alk = 4×10^{-4} eq/L, $\Sigma CO_2 = 1.0 \times 10^{-3}$ M, Σ"CH_2O" = 2×10^{-4} M, pH = 6.3. Determine the pH, pε, and speciation of sulfur and iron when all organic matter is consumed and redox equilibrium is achieved. The first dissociation constant of H_2S is 10^{-7}.

Answer: Let's first consider the redox reactions involved. The species involved in redox reactions will be those of carbon, sulfur, and iron. The concentration of iron is small, so its oxidation state will reflect, rather than control, that of the solution. Thus oxidation of organic matter will occur though reduction of sulfate. We can express this by combining reactions 7 and 11 in Table 13.1 (we see from the dissociation constant that H_2S will be the dominant sulfate species at pH below 7, so we chose reaction 7 rather than reaction 8):

$$\frac{1}{2}SO_4^{2-} + H^+ + CH_2O \rightleftarrows \frac{1}{2}H_2S + H_2O + CO_2 \qquad K=10^{10.54} \qquad 13.9$$

From the magnitude of the equilibrium constant (obtained from the pε°'s in Table 13.1), we can see that right side of this reaction is strongly favored. Since sulfate is present in excess of organic matter, this means sulfate will be reduced until all organic matter is consumed, which will leave equilmolar concentrations of sulfate and sulfide (10^{-4} M each). Thus the redox state of the system will be governed by that of sulfur. The redox state of iron can then be related to that of sulfur using reaction 13.8, for which we calculate an equilibrium constant of $10^{-10.75}$ from Table 13.1.

The next problem we face is that of chosing components. As usual, we chose H^+ as one component (and implicitly H_2O as another). We will also want to chose a sulfur, carbon, and iron species as a component, but which ones? We could chose the electron as a component, but consistent with our conclusion above that the redox state of the system is governed by that of sulfur, a better choice is to chose both sulfate and sulfide, specifically H_2S, as components. We can also see from Table 13.1 that Fe should be largely reduced, so we chose Fe^{2+} as the iron species. pH will be largely controlled by carbonate species, since these are more than an order of magnitude more abundant than sulfate species; oxidation of organic matter will increase the concentration of CO_2, which will lower pH slightly. In

Figure 6.1, we can see that at pH below 6.4, H_2CO_3 will be the dominant carbonate species, so we chose this as the carbonate species. Our components are therefore H^+, SO_4, H_2CO_3, Fe^{2+}, and H_2S. The species of interest will include H^+, OH^-, SO_4^{2-}, H_2S, HS^-, H_2CO_3, HCO_3^-, as well as the various species of Fe (Fe^{2+}, Fe^{3+}, $Fe(OH)^{2+}$, $Fe(OH)_2^+$, $Fe(OH)_3$ (we assume that the concentrations of CO_3^{2-}, HSO_4^- and S^{2-} are neglible at this pH; we shall neglect them throughout).

Our next step is to determine pH. For *TOT*H we have:

$$TOTH = [H^+] - [OH^-] - [HCO_3^-] - [HS^-] + \frac{5}{4}\Sigma Fe^{3+} \qquad 13.10$$

The presence of the Fe^{3+} term may at first be confusing. To understand why it occurs, we can use equation 13.7 to express Fe^{3+} as the algebraic sum of our components:

$$Fe^{3+} = \frac{1}{8}SO_4^{2-} + \frac{5}{4}H^+ + Fe^{2+} - \frac{1}{8}H_2S + \frac{1}{2}H_2O \qquad 13.11$$

The first 4 terms on the right hand side of equation 13.10 are simply alkalinity plus additional CO_2 produced by oxidation of organic matter, so 13.10 may be rewritten as:

$$TOTH = \frac{5}{4}\Sigma Fe^{3+} - Alk - [CH_2O] \qquad 13.12$$

Inspecting equation 13.10, we see that HCO_3^- is by far the largest term. Furthermore, the Fe term in equation 13.12 is neglible, so we have:

$$TOTH \simeq -[HCO_3^-] \simeq 6 \times 10^{-4} \qquad 13.13$$

The conservation equation for carbonate is:

$$\Sigma H_2CO_3 = [H_2CO_3] + [HCO_3^-] = \Sigma CO_2 + \Sigma[CH_2O] = 1.3 \times 10^{-3}$$

Hence: $$H_2CO_3 = \Sigma H_2CO_3 - HCO_3^- = (1.3 - 0.6) \times 10^{-3}$$

We can use this to calculate pH since: $$K = [\frac{HCO_3^-][H^+]}{[H_2CO_3]} = 10^{-6.35}$$

Solving for $[H^+]$ and substitutiong values, we find that pH = 6.28.

For the conservation equation for sulfate, we will have to include terms for both Fe^{3+} (equation 13.11) and organic matter. Writing organic matter as the algebraic sum of our components we have:

$$CH_2O = \frac{1}{2}H_2S + H_2O + CO_2 - \frac{1}{2}SO_4^{2-} - H^+$$

The amount of sulfate present will be that originally present less that used to oxidize organic matter. The only other oxidant present in the system is ferric iron, so the amount of sulfide used to oxidize organic matter will be the total organic matter less the amount of ferric iron initially present. The sulfate conservation equation is then:

$$\Sigma SO_4 = [SO_4^{2-}] - \frac{1}{2}\Sigma CH_2O + \frac{1}{8}\Sigma Fe^{3+} \simeq 1.0 \times 10^{-4}\ M$$

(the Fe term is again neglible). The amount of sulfide present will be the amount created by oxidation of organic matter, less the amount of organic matter oxidized by iron, so the sulfide conservation equation is:

$$\Sigma H_2S = H_2S + HS^- = + \frac{1}{2}\Sigma CH_2O - \frac{1}{8}\Sigma Fe^{3+} = 1 \times 10^{-4}\ M \qquad 13.14$$

We now want to calculate the speciation of sulfide. We have

$$\Sigma H_2S = H_2S + HS^- = 1 \times 10^{-4}\ M \qquad \text{and} \qquad K_{1H_2S} = \frac{[H^+][HS^-]}{[H_2S]} = 10^{-7}$$

Solving these two equations, we have:

$$[HS^-] = \frac{10^{-4}}{10^7 10^{-6.23}} = 1.92 \times 10^{-5}$$

The concentration of H_2S is then easily calculated as 8.08×10^{-5} M. We can now calculate the pε of the solution by substituting the above values and the pε° in Table 13.1 for reaction 7 into equation 13.7. Doing so, we find pε is -2.72. Finally, for iron we have:

$$\Sigma Fe = [Fe^{2+}] + \Sigma[Fe^{3+}] = 10^{-6} \quad \text{and} \quad \log \frac{[Fe^{2+}]}{[Fe^{3+}]} = p\varepsilon - p\varepsilon^\circ = -2.72 - 13.0 = 15.78 \qquad 13.15$$

so that $Fe^{2+} = 10^{15.78}Fe^{3+}$. The equilibrium concentrations of the hydrolysis species of Fe^{3+} can be calculated from equations 6.73a through 6.73d. We find the most abundant species will be $Fe(OH)_2^+$, which is $10^{6.8}$ times more abundant than Fe^{3+}. However, Fe^{2+} remains $10^{15.78} \times 10^{-6.9}$ more abundant that $Fe(OH)_2^+$, so for all practical purposes, all iron is present as Fe^{2+}.

The development of anoxic conditions leads to an interesting cycling of iron and manganese within the water column. Below the oxic-anoxic boundary, Mn and Fe in particulates are reduced and dissolved. The metals then diffuse upward to the oxic-anoxic boundary where they again are oxidized and precipitate. The particulates then migrate downward, are reduced, and the cycle begins again.

A related phenomena can occur within sediments. Even where anoxic conditions are not achieved within the water column, they can be achieved within the underlying sediment. Indeed, this will occur where burial rate of organic matter is high enough to exceed the supply of oxygen. Figure 13.3 shows an example, namely a sediment core from southern Lake Michigan studied by Robbins and Callender (1975). The sediment contains about 2% organic carbon in the upper few centimeters, which decreases by a factor of 3 down core. The concentration of acid-extractable Mn in the solid phase (Figure 13.3a), presumably surface-bound Mn and Mn oxides, is constant at about 540 ppm in the upper 6 cm, but decreases rapidly to about 400 ppm by 12 cm. The concentration of dissolved Mn in the pore water increases from about 0.5 ppm to a maximum of 1.35 ppm at 5 cm and then subsuquently decreases (Figure 13.3) to a constant value of about 0.6 ppm in the bottom half of the core.

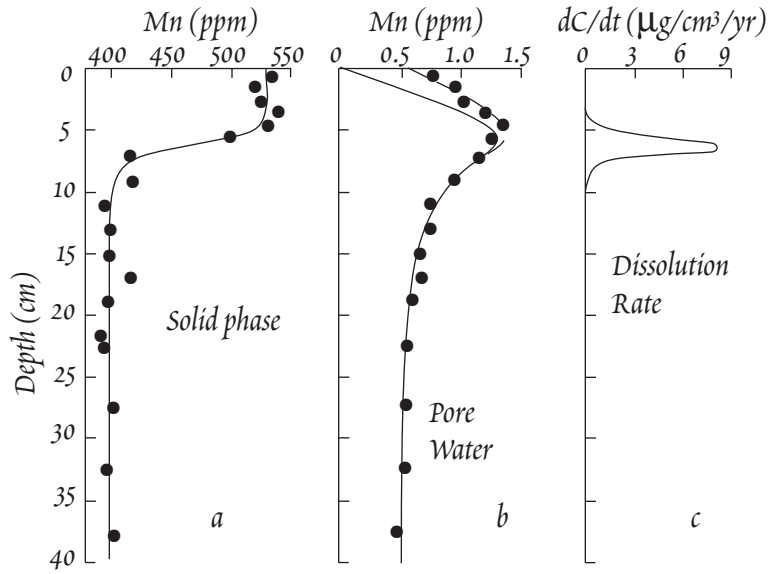

Figure 13.3. (a) Concentration of acid-leachable Mn in Lake Michigan sediment as a function of depth. (b) (b) Dissolved Mn in pore water from the same sediment core. Solid line shows the dissolution-diffusion-reprecipitation model of Robbins and Calender (1975) constrained to pass through 0 concentration at 0 depth. Dashed line shows the model when this constraint is removed. (c) Dissolution rate of solid Mn calculated from rate of change of concentration of acid-leachable Mn and used to produce the model in (b). From Robbins and Calender (1975).

Because the Lake Michigan region is heavily populated, it is tempting to interpret the data in Figure 13.3, particularly the increase in acid-extractable Mn near the core top, as being a result of recent pollution. However, Robbins and Callender (1975) demonstrated that the data could be explained with a simple steady-state diagentic model involving Mn reduction, diffusion, and reprecipitation (as $MnCO_3$). In Chapter 5, we derived the Diagenetic Equation:

$$\left(\frac{\partial c}{\partial t}\right)_x = \left(\frac{\partial F}{\partial x}\right)_t + \sum R_i \qquad (5.171)$$

The first term on the right is the change in total vertical flux with depth, the second is the sum of rates of all reactions occuring. There are two potential flux

terms in this case, pore water advection (due ot compaction) and diffusion. There are also several reaction occurring: dissolution or desorption associated with reduction and a precipitation reaction. If the system is at steady state, then $\partial c/\partial x = 0$. Assuming steady-state, Robbins and Callender (1975) derived the following verision of the diagenetic equation:

$$\phi D \frac{d^2c}{dx^2} - v \frac{dc}{dx} - \phi k_1 (c - c_f) + \phi k_0(z) = 0 \qquad 13.16$$

where ϕ is porosity (assumed to be 0.8), D is the diffusion coefficient, v is the advective velocity (-0.2 cm/yr), and k_1 is the rate constant for reprecipitation reactions, and k_0 is the dissolution rate (expressed as a function of depth). The first term is the diffusive term, the second the advective, the third the rate of reprecipitation, and the fourth is the dissolution rate. The dissolution rate must be related to the change in concentration of acid-extractable Mn. Thus the last term may be written as:

$$\phi k_0(z) = \phi \frac{R}{\phi} \frac{\partial c_s}{\partial x}$$

where R is the sedimentation rate (g/cm^2/yr) and c_s is the concentration in the solid. Using least squares, Robbins and Callender found that the parameters that best fit the data were $D = 9 \times 10^{-7}$ cm^2/sec (30 cm^2/yr) $k_1 = 1$ yr^{-1} and $c_f = 0.5$ ppm. The solid line in Figure 12.44b represents the prediction of equation 13.16 using this values and assuming c_0 (porewater concentration at the surface) is 0. The dashed line in Figure 13.3b assumes $c_0 = 0.6$ ppm. The latter is too high, as c_0 should be the same concentration as lake water. Robbins and Callender (1975) speculated that the top cm or so of the core had been lost, resulting in an artifically high c_0.

Redox cycling, both in water and sediment can effect the concentrations of other a number of other elements. For example, Cu and Ni form highly insoluble sulfides. Once pε decreases to levels where sulfate is reduced to sulfide, dissolved concentrations of Cu and Ni decrease dramatically due to sulfide precipitation. The dissolved concentrations of elements that are strongly absorbed onto particulate Mn and Fe oxihydroxide surfaces, such as the rare earths and P, often show significant increases when these particulates dissolved as Mn and Fe are reduced. The effect of Fe redox cycling on P is particularly significant because P is most often the nutrient whose availability limites biological productivity in freshwater ecosystems. Under oxic conditions, a fraction of the P released by decomposition of organic matter in deep water or sediment will be adsorbed by particles (particularly Fe) and hence lost from the ecosystem to sediment. If conditions become anoxic, iron dissolves and adsorbed P is released into solution, where it can again become available to the biota. As a result, lakes that become eutrophic due to P pollution can remain so long after the the pollution ceases because P is simply internally recycled under the prevailing anoxic conditions. Worse yet, once conditions become anoxic, nonanthropogenic P can be released from the sediment, leading to higher biological production and more severe anoxia.

Weathering, Soils, and Biogeochemical Cycling

Weathering is the process by which rock is physically and chemically broken down into relatively fine solids (soil or sediment particles) and dissolved components. The chemical component of weathering, which will be our focus, could be more precisely described as the process by which rocks originally formed at higher temperatures come to equilibrium with water at temperatures prevailing at the the surface of the Earth.

Weathering plays a key role in the *exogenic* geochemical cycle (i.e., the cycle operating at the surface of the Earth). Chemical weathering supplies both dissolved and suspended matter to rivers and seas. It is the prinicipal reason that the ocean is salty. Weathering also supplies nutrients to the biota in form of dissolved components in the soil solution; without weathering terrestrial life would be far different and far more limited. Weathering can be an important source of ores. The Al ore bauxite is the product of extreme weathering that leaves a soil residue containing very high concentrations of aluminum oxides and hydroxides. Weathering, together with erosion, transforms the surface of the Earth, smoothing out the roughness created by volcanism and tectonism.

CHAPTER 13: WEATHERING, SOILS, AND STREAM CHEMISTRY

Geochemists are particularly concerned with question of what controls weathering rates. This concern arises from both the role weathering plays as a sink for atmospheric CO_2 and the variety of anthropogenic activities that influence weathering rates. Agriculture and harvesting of forests have had a clear impact on erosion, and probably chemical weathering rates as well. Combustion products of fossil fuels released to the atmosphere include nitrates and sulfates that acidify precipitation ("acid rain"). The resulting decrease in pH has had a clear adverse effect on the biota in some localities and may also affect chemical weathering rates. On the other hand, weathering consumes H^+ and thereby increases pH; in some localities this buffering effect of weathering reactions is sufficient to entirely overcome the effects of acid rain. Understanding the impact of acid rain and the degree to which its effects are mitigated by weathering is an important goal of many weathering studies.

Weathering, and the subsequent precipitation of carbonate in the ocean, also consumes CO_2 in reactions such as:

$$CaAl_2Si_2O_8 + H_2CO_3 + 3H_2O \rightleftarrows CaCO_3 + Al_2Si_2O_5(OH)_4$$

Weathering thus appears to be an important control on the concentration of atmospheric CO_2, which is in turn an important control on global temperature and climate. Hence whatever factors control the weathering rate may also control climate. What are these factors? In the BLAG (Berner Lasaga and Garrels) model of atmospheric CO_2 levels over geological time, Berner et al. (1983) and Berner (1991) assumed that temperature is a strong control on weathering rate, and therefore that there is a negative feedback that controls atmospheric CO_2 levels (the higher the atmospheric CO_2, the higher the global temperature, the higher the weathering rate, and therefore the higher the consumption of atmospheric CO_2). Others, including Edmond et al. (1995), have argued that despite the odvious temperature effect on reaction rates, global temperature exerts little control on weathering rates in nature, and that tectonic uplift and exposure of fresh rock has a much stronger influence on weathering rate, and ultimately on global climate.

In previous chapters and sections, we examined many important weathering reactions from thermodynamic and kinetic perpectives. In this section, we will step back to look at weathering on a broader scale and examine weathering in nature and the interrelationships among chemical weathering, biological processes, and soil formation. We then discuss in some detail the question of what controls on weathering rates. Finally, we look at the composition of rivers and streams.

Most rock at the surface of the Earth is overlain by a thin veneer of a mixture of weathering products and organic matter that we refer to as soil. Most weathering reactions occur within the soil, or at the interface between the soil and bedrock, so it is worth briefly considering soil and its development. Soil typically consists of a sequence of layers that constitute the soil profile (Figure 13.4). The nature of these layers varies, depending on climate (temperature, amount of precipitation, etc.), vegetation (which in turn depends largely on climate), time, and the nature of the underlying rock. Consequently, no two soil profiles will be identical. What follows is a general description of an idealized soil profile. Real profiles, as we shall see, are likely to differ in some respects from this.

Soil Profiles

The uppermost soil layer, referred to as the *O horizon*, consists entirely, or nearly so, of organic material whose state of decomposition increases downward. This layer is best developed in forested regions or waterlogged soils depleted in O_2 where decomposition is slow. In other regions it may be incompletely developed or entirely absent.

Below this organic layer lies the upper mineral soil, designated as the *A horizon* or the zone of removal, which ranges in thickness from several centimeters to a meter or more. In addition to a variety of minerals, this layer contains a substantial organic fraction, which is dominated by an amorphous mixture of unsoluble, refractory organic substances collectively called *humus*. Weathering reactions in this layer produce a soil solution rich in silica and alkali and alkaline earth cations that percolates downward into the underlying layer. In temperate forested regions, where rainfall is high and organic decomposition slow, Fe and Al released by weathering reactions are complexed by organic

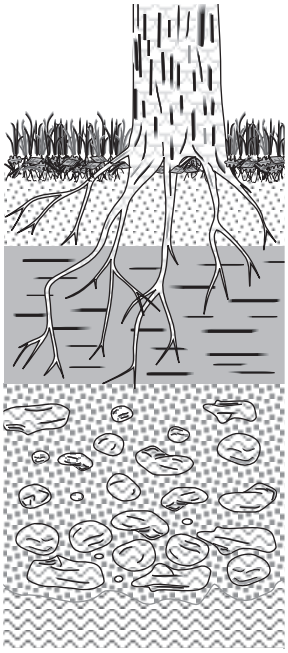

Figure 13.4. Soil profile, illustrating the O, A, B, and C horizons described in the text. Not all soils comform to this pattern.

(fulvic) acids and carried downward into the underlying layer. The downward transport of Fe and Al is known as *podzolization*. In tropical regions, organic decomposition is sufficiently rapid and complete that there is little available soluble organic acid to complex and transport Fe and Al, so podzolization may not occur. As a result, Fe and Al accumlate in the A horizon as hydrous oxides and hydroxides. Where leaching is particularly strong, the A horizon may be underlain by a thin whitish highly leached, or eluviated, layer known as the *E horizon*, enriched in highly resistant minerals such as quartz. In grasslands and deserts, the production of soluble organic acids is restricted by the availability of water, hence the podzolization is limited.

The *B horizon*, or zone of accumulation or deposition, underlies the A horizon. This horizon is richer in clays and poorer in organic matter than the overlying A horizon. Substances leached from the A horizon are deposited in this B horizon. Fe and Al carried downward as organic complexes precipitate here as hydrous oxides and hydroxides, and may react with other components in the soil solution to form other secondary minerals such as clays. In arid regions where evaporation exceeds precipitation, relatively soluble salts such as calcite, gypsum, and halite precipitate within the soil. Downward percolating water leaches these from the A horizon and concentrates them within in the B horizon. Such calcite layers are known as *caliche*, and are typically found at a depth of 30 to 70 cm. The clay-rich nature of the B horizon, particularly when cemented by precipitated calcite or Fe oxides, can lead to greatly restrict permeability of this layer. Such impermeable layers are sometimes referred to as *hardpan*. In tropical regions, where weathering is intense and has continued for millions of years in the absence of disturbances such as glaciation, the soil profile maybe up to 100 m thick. Because of the absence of podzolization, there is often little distinction between the A and B horizons. Base cations are nearly completely leached in tropical soils, leaving a soil dominated by minerals such as kaolinite, gibbsite, and Fe oxides. Such soils are called *laterites*. In the most extreme cases, SiO_2 maybe nearly completely leached as well, leaving a soil dominated by gibbsite. The ratio of SiO_2 to Al_2O_3 + Fe_2O_3 (collectively called the sesquioxides) is a useful index of the intensity of weathering within the soil as well as to the extent of podzolization. Typical values for the A and B horizons of several climatic regions are summarized in Table 13.2. Often, seperate layers can be recognized within the B and the other horizons and these are designated B_1, B_2, etc. downward.

The *C horizon* underlies the B horizon and directly overlies the bedrock. It consists of partly weathered rock, often only coarsely fragmented, and its direct weathering products. Very often it consists of *saprolite*, rock in which readily weatherable silicates have been largely or wholy replaced *in situ* by clays and oxides, but textures and structures are often sufficiently well preserved that the nature of the original parent maybe recognized. This

TABLE 13.2. $SiO_2/(Al_2O_3 + Fe_2O_3)$ RATIOS OF SOILS

	A horizon	B horizon
Boreal	9.3	6.7
Cool-temperate	4.07	2.28
Warm-temperate	3.77	3.15
Tropical	1.47	1.61

From Schlesinger (1991).

layer has relatively little organic matter. In soils that develop directly from local materials, it is mineralogically related to the underlying bedrock. Alternatively, soil may develop on volanic ash, glacial till, or material transported by wind (loess) or water (alluvium). Loess up to 100 m thick was deposited in some northern regions during the Pliestocene glaciations. Soils in deserts surrounded by mountains and in river floodplains generally develop from alluvium rather than underlying bedrock. In such cases, the C layer will be unrelated to underlying bedrock or may be underlain by fossil soils (paleosols). While organic acids dominate weathering reactions in the upper part of the soil profile, carbonic acid, produced by respiration within the soil and transported downward by percolating water, is largely responsible for weathering in the C horizon.

The full development of an "equilibrium" soil profile requires time, thousands to hundreds of thousands of years. How much time depends largely on climate: soil development is most rapid in areas of warm temperature and high rainfall. Regions that have been disturbed in the recent geologic past may show incomplete soil formation, or soils uncharacteristic of the present climate. For example, many desert soils contain clay layers developed during wetter Pleistocene times. Soils in recently glaciated areas of North America and Europe remain thin and immature, even though 12,000 years have past since the last glacial retreat. Floods and landslides are other natural processes that can interupt soil development. Soil profiles are also be disturbed by agriculture and the resulting increase in erosion and other anthropogenic effects such as acid rain. Thus actual soil profiles often deviate from that illustrated in Figure 13.4.

Chemical Cycling in Soils

An example of chemical variations in a soil profile is shown in Figure 13.5. This soil, developed on a beach terrace in Mendocino County, California, was studied by Brimhall and Dietrich (1987) and illustrates processes occuring in a podzol (a soil that has experienced podzolization). The parent material is Pleistocene beach sand and is poor in most elements other than Si compared to common rocks. The soil profile consists of an A horizon, the upper part of which is densely rooted and rich in organic matter, unlain by a transitional layer that Brimhall and Dietrich (1987) labelled Bmir. This is in turn underlain by a white and red banded E horizon, which is in turn unlain by the B horizon, which Brimhall and Dietrich (1987) divided into B1 and B2 layers based on appearance.

Figure 12.46 shows that Fe and Al are slightly, though not uniformly, depleted from the surface through the E horizon, and strongly enriched in the B horizon. This reflects the downward transport of these element as organic complexes. Si is present in roughly the same concentrations as in the parent through the E horizon, and relatively depleted in the underlying B horizons. Though Si has undoubtedly been leached throughout the profile, the leaching has been more severe for other elements than for Si in the upper profile, leaving the Si concentration nearly unchanged. The lower concentrations in the lower horizon in part reflects dilution by Fe and Al. The alkalis and alkaline earths are depleted thoughout the profile relative to the parent, but while Na and Ca are uniformly depleted (as is Sr, not shown in the Figure), K, Rb, and Ba are enriched in the B horizon. These elements are all readily soluble and hence easily leached in the upper part of the soil profile, but K, Rb, and Ba are readily accepted in the interlayer sites of clays. Thus clay formation probably explains the enrichment of these elements in the B horizon. The profiles of Pb, Cu (not shown), and Ga resemble that of K (though they are also somewhat enriched at the base of the A horizon). Brimhall and Dietrich (1987) speculated that this is due to oxidation of sulfides in the upper horizon, downward transport as organic complexes, and reprecipitation as sulfides in the B horizon. Ti and Nb, as well as Zr (not shown) are present in concentrations greater than that of the parent throughout most of the profile. These elements are not soluble and do not form soluble complexes hence they are virtually immobile in soil profiles. Their apparent enrichment is due entirely to the loss of other elements. Indeed, Brimhall and Dietrich use Nb and Ti concentrations to calculate that there is been a mass loss, through leaching, of 60% in the upper part of the soil profile.

From the preceeding discussion, we can infer that considerable chemical cycling occurs within soils. The initial stages of weathering occur within the C horizon, where the most unstable primary miner-

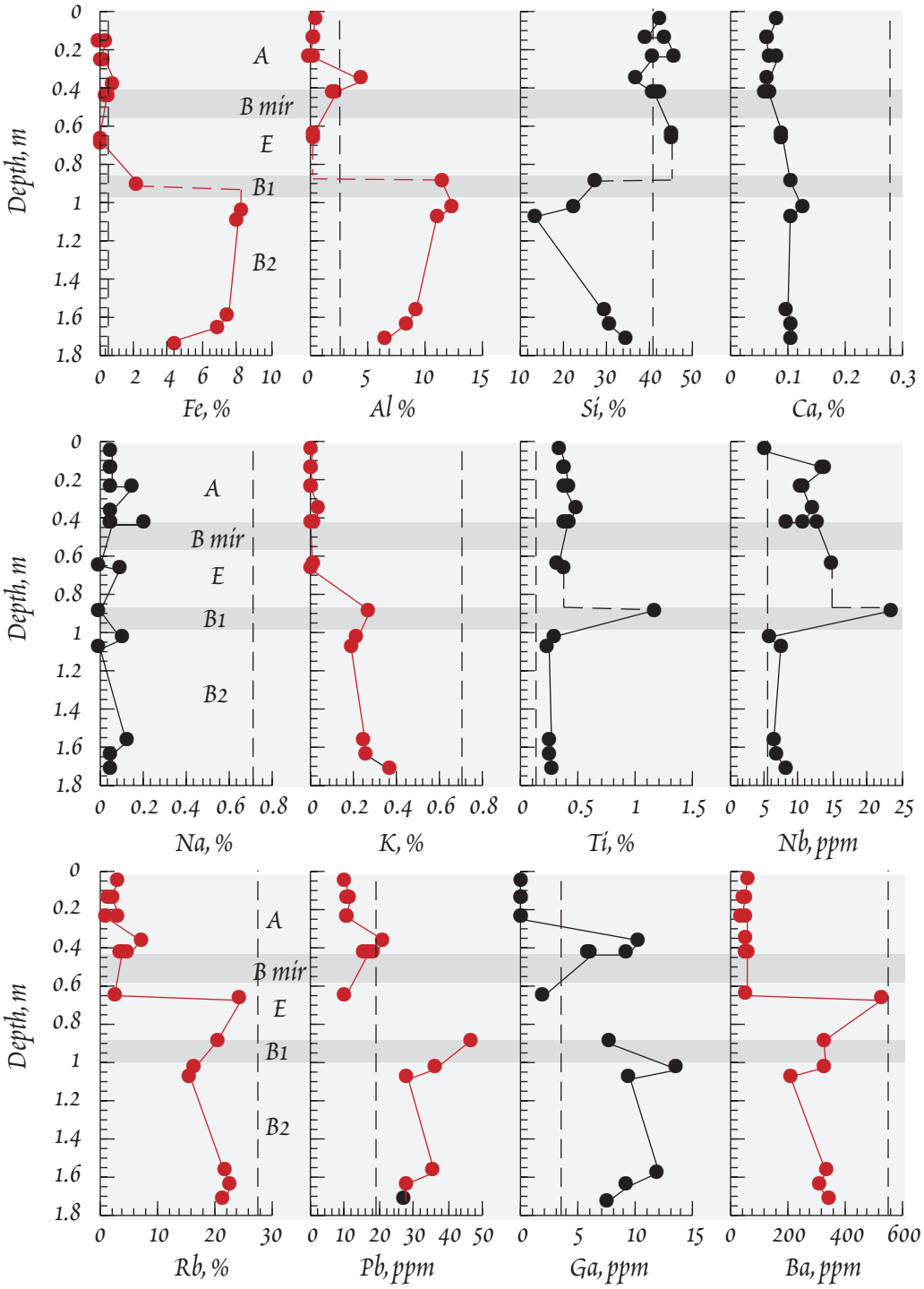

Figure 13.5. Concentration profiles in a podzol developed on a Pleistocene beach terrace in Mendicino, California. Dashed line shows the concentration in the parent beach sand. Soil horizons are simplified from those identified by Brimhall and Dietrich (1987). Data from Brimhall and Dietrich (1987).

als (e.g., sulfides, carbonates, feldspars, ferromagnesian silicates such as olivine, pyroxenes, amphiboles) undergo reaction. More resistant minerals such as quartz and Fe-Ti oxides may remain largely intact at this stage. A substantial fraction of the more soluble elements, such as the alkalis and alkaline earths, may be lost to solution at this stage. As erosion slowly lowers the surface, minerals in the C horizon are, in effect, transported into the B horizon. At this stage, new secondary minerals form by precipitation from and reaction with downward percolating solutions. In areas of high rainfall, the most important of these are Fe and Al oxihydroxides; in arid regions, carbonates and sulfates may be the dominant new minerals forming in the B horizon. Further leaching and loss of readily soluble elements, as well as SiO_2, will continue in this stage in humid climates. As erosion continues to lower the surface, the material will eventually reach the A horizon. Here, many of the secondary minerals formed in the C and B horizons breakdown, releasing their components to solution. Some of the material leached from this horizon will reprecipitate in the B horizon and some will be lost to groundwater and streams. In addition, plants actively take up dissolved consitutents from the soil solution and store it within their tissues. These constituents will be returned to the soil when the tissue dies and is broken down by bacteria. Thus in principle, an element might be cycled many times between the biota, and the O, A, and B horizons before being carried away in groundwater flow.

Biogeochemical Cycling

The biota plays a substantial role in the weathering process and in controlling the composition of streams. As we saw earlier in this chapter, P_{CO_2} is substantially higher in soil than in the atmosphere; this is a direct result of respiration of organisms in the soil. This higher P_{CO_2} lowers pH and hence accelerates weathering reactions. Organic acids produced by plants and bacteria have the same effect. In addition, many weathering reactions, including, but not limited to, redox reactions, may be directly catalyzed by soil bateria. Plants also take up a host of elements released by rock weathering as nutrients. The biota will thus influence both soil and water chemistry within a watershed and can be a significant reservoir for some elements.

Living organisms consist of a bewildering variety of organic compounds (we will discuss some of these is Chapter 13). From a geochemical perspective, it is often satisfactory to approximate the composition of the biomass as CH_2O (for example the composition of glucose, a simple sugar, is $C_6H_{12}O_6$). A better approximation for the composition of land plants would be $C_{1200}H_{1900}O_{900}N_{25}P_2S_1$ (Berner and Berner, 1996). A great many other nutrients*, however, are essential for life (for example, Mg and Fe are essential photosynthesis; Mo is essential for nitrate reduction) and are taken up by plants in smaller amounts. These can be divided up into *macronutrients*, which occur in plants at concentrations in excess of 500 ppm and include N, P, K, Ca, Mg, and S, and *micronutrients*, which occur at lower concentrations and include B, Fe, Mn, Cu, Zn, Mo, Co, and Cl. Other elements are also taken up by plants and stored in tissue even though they play no biochemical role (so far as we know), simply because plants cannot discriminate sufficiently against them. Table 13.3 lists the concentrations of the elements in dried plant matter. One should be aware, however, that the actual composition of plants varies widely; grasses, for example, can contain over 1% SiO_2 (>4600 ppm Si).

Table 13.3. Elemental Composition of Dried Plant Matter

Element	Percent	Element	ppm
C	49.65	V	1
N	0.92	Mn	400
O	43.2	Cr	2.4
Total	93.77	Fe	500
Element	ppm	Co	0.4
Li	0.1	Ni	3
B	5	Cu	9
Na	200	Zn	70
Mg	700	Se	0.1
Al	20	Rb	2
Si	1500	Sr	20
P	700	Mo	0.65
S	500	Ag	0.05
K	3000	Ba	30
Ca	5000	U	0.05
Ti	2		

From Brooks (1972).

* A nutrient as an element or compound essential to life that cannot be synthesized by the organism and therefore must be obtained from an external source.

Chapter 13: Weathering, Soils, and Stream Chemistry

There are four sources of nutrients in an ecosystem: the atmosphere, dead organic matter, water, and rock. The atmosphere is the obvious direct source of CO_2 and O_2 and the indirect source of N and H_2O in terrestrial ecosystems. However, it may also be the direct or indirect source of a number of other nutrients, which arrive either in atmospheric dust or dissolved in rain. Plants are able to take up some of these atmosphere-delivered nutrients directly through foliage; most, however, cycle through the soil solution and are taken up by roots, which is the primary source of nutrients. Plants cannot take up nutrients from dead organic matter or from rocks directly: nutrients from these sources must first be dissolved in the soil solution. Because equilibrium between surface adsorbed and dissolved species is achieved relatively quickly, elements adsorbed on the surfaces of oxides, clays, and organic solids represent an intermediate reservoir of nutrients. For example, phosphrous, often the growth-limiting nutrient, is readily adsorbed on the surface of iron oxides and hydroxides. For this reason, the surface properties of soil particles are an important influence on soil fertility. Even in relatively fertile soils, however, the concentration of key nutrients such as phosphorous may be effectively zero in the soil immediately adjacent roots, and the rate of delivery to plant may be limited by diffusion.

In most ecosystems, particularly mature ones, detritus, that is dead organic matter, is the the most important source of nutrients. In the Hubbard Brook Experimental Forest, for example, this recycling supplies over 80% of the required P, K, Ca, and Mg (Schlesinger, 1991). For the most part, this recycling occurs as leaf tissue dies, falls to the ground, and decomposes. However, some fraction of nutrients are recycled more directly. Nutrients may be leached from leaves by precipitation, a process called *translocation*. Translocation is particularly important for K, which is highly soluble and concentrated in cells near the leaf surface, but it can be important for other elements as well. Nutrient loss from leaves by leaching increases in the order K>>P>N>Ca. In addition to nutrient recycling through translocation and detritus, plants also recycle nutrients internally by withdrawing them from leafs and stems before the annual loss of this material and storing them for use in the following season. For this reason, the concentration of nutrients in litterfall is lower than in living tissue. Not surprisingly, the fraction of nutrients recycled in this way, and overall nutrient use efficiency, is higher in plants living on nutrient-poor soils (Schlesinger, 1991).

Rainwater passing through the vegetation canopy will carry not only nutrients leached from foliage, but also species dissolved from dust and aerosols (together called dry deposition) deposited on leaves. Fog and mist will also deposit solutes on plant leaves. The term *occult* deposition refers to both dry deposition and deposition from mist and fog. The total flux of solutes dissolved from leaf surfaces, including both the occult deposition and translocation fluxes, and carried to the soil by precipitation is called *throughfall*, and can be quite significant in regions where there is a high aerosol flux. Such regions may be either those downwind from heavily populated areas, where the atmosphere contains high levels of nitrate and sulfate from fossil fuel burning, or arid regions, where there is abundant dust in the atmosphere. Table 13.4 compares the concentration of nutrients measured in

Table 13.4. Concentrations in Bulk Precipitation and Throughfall in the Vosage, France

	NH_4	Na	K	Mg	Ca	H^+	Cl	NO_3	SO_4
Concentration (μeq/L)									
Bulk precipitation	19.1	10.0	2.8	4.5	11.9	33.9	12.5	24.1	41.5
Throughfall	36.9	46.4	52.7	17.8	65.5	114.8	63.4	48.3	185.0
Fluxes (moles/ha/y)									
Bulk precipitation	270.0	142.0	39.0	32.0	84.0	480.0	177.0	340.0	290.0
Throughfall	385.0	484.0	550.0	93.0	642.0	1197.0	661.0	817.0	966.0
Difference	115.0	342.0	511.0	61.0	558.0	717.0	484.0	477.0	676.0
Occult precipitation	115.0	342.0	102.0	31.0	206.0	1282.0	484.0	477.0	676.0
Translocation	0.0	0.0	409.0	30.0	352.0	-565.0	0.0	0.0	0.0

Data from Probst et al. (1990).

throughfall and bulk precipitation, and demonstrates the importance of translocation and occult deposition.

The biota affects the composition of soil and stream water in another way as well. Some fraction of soil water taken up by roots is ultimately lost from the plant to the atmosphere through leaf stomata, the opening designed to allow CO_2 into the leaf. This loss of water is called *transpiration*. Water lost through transpiration and that lost by direct evaporation from the ground surface are often collectively called *evapotranspiration*. As one might expect, transpiration varies seasonally: transpiration is high in spring and summer when plants are actively growing and stomata are open and minimal in winter. Transpiration also depends on climatic factors such as temperature and relative humidity, as does evaporation. Evaptranspiration concentrates dissolved solids in soil and stream water.

Table 13.5. Residence Times of Organic Matter and Nutrients in Forest Litter

Region	Organic Matter	N	P	K	Ca	Mg
Boreal forest	353	230	324	94	149	455
Temperate forest						
coniferous	17	17.9	15.3	2.2	5.9	12.9
diciduous	4	5.5	5.8	1.3	3	3.4
Meditteranean	3.8	4.2	3.6	1.4	5	2.8
Tropical rainforest	0.4	2	1.6	0.7	1.5	1.1

From Schlesinger (1991).

Dead vegegtation lying above the mineral soil (the O soil horizon) is called *litter*. The rate at which litter decomposes, and hence "turns over" depends strongly on climate. Table 13.5 lists the mean residence times of bulk organic matter and nutrients in the surface litter of forest ecosystems. The great range of times, from hundreds of years in boreal forests to a year or less in tropical rainforests, is particularly interesting. K is recycled more rapidly than bulk organic matter, but recycling times for other nutrients are generally comparable to that of bulk organic matter. Though animals, particularly those living in the soil such as termites and worms, play a role in organic decomposition, most of it is carried out by soil fungi and bacteria. These soil microbes can comprise up to 5% of the organic carbon in soils, with fungi dominating over bacteria in well-drained soils. Decomposition of organic matter is acomplished by extracellular enzymes released by these organisms. Because soil microbes concentrate them, a particularly high fraction of organicly bound N and P in soils is contained in the microbial biomass.

As microbes decompose organic matter, they preferentially oxidize the most labile, energy-rich compounds, such as sugars, and synthesize humus from refractory compounds such as lignins and tannins. Soil humus together with humic and fulvic acids, which are closely related (see Chapter 13), accumulate within the soil. As we have mentioned, the cation exchange capacity of this soil organic matter is important, both in providing a reservoir of nutrients to plants, and also in downward transport of Al and Fe in soils. In most cases, the mass of soil humus exceeds the combined mass or living vegetation and litter. The residence time humus in the soil may exceed that of litter by several orders of magnitude, with measured mean ^{14}C ages ranging upward to thousands of years.

Weathering Rates and Reactions

The Watershed Approach

As we stated at the beginning of this section, weathering produces two products: secondary minerals and dissolved components. The process may be studied in a variety of ways and on a variety of scales. Perhaps the most basic study is simply to observe the phase that replace original ones as weathering of exposed rock proceeds. These observations providing the starting point for laboratory experiments from which thermodynamic and kinetic data may be deduced. A third approach, and the one we explore in this section, looks at the problem on a much larger scale: that of a watershed. This approach relies on the observation that mass is conserved in weathering reactions (like any other chemical reaction). Mathematically, we may write the following mass balance equation:

rock + rain = altered rock + solution

Thus if the composition of the original rock, input composition (bulk precipitation and occult precipitation), and the final water composition (the dissolved component) are known, then the gross composition of the secondary phases can be calculated. This point is illustrated in Figure 13.6. Such an approach ignores considerable complexity and details, such as the geochemical and biogeochemical cycling that occurs in the soil and biota. Often, a key assumption in such studies is that the system is at *steady-state*; if so, any internal cycling will not affect the net output of the system. It is, however, not always clear that the assumption of steady-state is valid, Nevertheless, such studies can be enormously useful in understanding weathering, particularly when it is combined with thermodynamics and kinetics to deduce the nature of weathering reactions occurring.

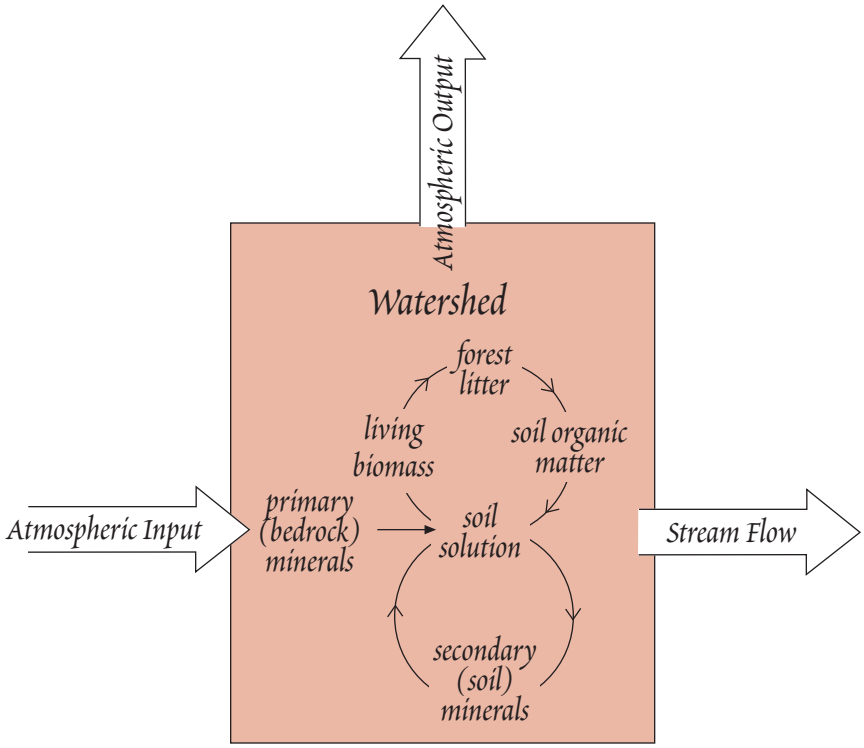

Figure 13.6. Illustrationof the mass balance approach to weathering on a watershed scale.

Spring Waters of the Sierra Nevada

The classic example of this type of study of is work of Feth et al. (1964) and Garrels and McKenzie (1967) on springs in the granitic terrane of the Sierra Nevada. Feth et al. (1964) measured concentrations of the principal constituents of perennial (those that always flowed) and ephemeral springs (springs that flowed only seasonally or after rain), and precipitation (atmospheric input). The data is summarized in Table 13.6. Garrels and McKenzie (1967) showed that composition of these waters could be explained by weathering of the local bedrock.

The granitic bedrock consists primarily of quartz, alkali feldspar, and andesine plagioclase with lesser amounts of hornblende and biotite. The primary weathering product observed was kaolinite. Garrels and McKenzie (1967) first subtracted from spring water the concentrations of ions found in snow. They then subtracted Na, Ca, HCO_3, and SiO_2 in proportions to convert kaolinite to plagioclase. Next all Mg and enough K were subtracted to make biotite, and the remaining K, HCO_3, and SiO_2 used to convert kaolinite to K-feldspar. For the ephemeral springs, this procedure produced mass balance within analytical error. In other words, the various ions were present in solution in the proportions expected from the reaction considered by Garrels and McKenzie.

The mass balance for the perennial springs was less satisfactory. They had higher total dissolved solids, higher pH and higher HCO_3, all of which indicated deeper circulation and more extensive interaction with rock, which is what one would expect. However, cation concentrations did not increase in the proportion expected if kaolinite were the only weathering product. In particular, the data suggested a more siliceous residual phase, as the increase in Na and SiO_2 in the perennial springs over

TABLE 13.6. AVERAGE CONCENTRATIONS OF DISSOLVED CONSTITUENTS IN SPRINGS OF THE SIERRA NEVADA (FROM GARRELS AND MCKENZIE, 1967).

	Ephemeral Springs		*Perennial Springs*	
	ppm	*molality* $\times 10^4$	*ppm*	*molality* $\times 10^4$
SiO_2	16.4	2.73	24.6	4.1
Al	0.03	—	0.018	—
Fe	0.03	—	0.031	—
Ca	3.11	0.78	10.4	2.6
Mg	0.70	0.29	1.70	0.71
Na	3.03	1.34	5.95	2.59
K	1.09	0.28	1.57	0.40
HCO_3	20.0	3.28	54.6	8.95
SO_4	1.00	0.10	2.38	0.25
Cl	0.50	0.14	1.06	0.30
F	0.70	—	0.09	—
NO_3	0.02	—	0.28	—
Σ Dissolved solids	36.0		75.0	
pH (median)	6.2		6.8	

the ephemeral springs was 1:1 whereas weathering of plagioclase to kaolinite releases Na and SiO_2 in 1:2 proportions. Smectite was a likely candidate.

The question of whether groundwater composition was controlled by a reaction between kaolinite and smectite (Ca-beidellite) can be addressed from a thermodynamic perspective. The reaction is:

$$3Ca_{0.33}Al_{4.67}Si_{7.33}O_{20}(OH)_4 + 2H^+ + 7H_2O \rightleftarrows 7Al_2Si_2O_5(OH)_4 + Ca^{2+} + 8SiO_{2(aq)} \qquad 13.17$$

The equilibrium constant for the reaction is:

$$K = \frac{a_{Ca^{2+}} a_{SiO_2(aq)}}{a^2_{H^+}} \qquad 13.18$$

A plot of the "reaction quotient", i.e., the right hand side of equation 13.18, against Na concentration is shown in Figure 13.7. As weathering proceeds, the composition of the solution should evolve along path ABD. On path ABC, Na and Ca are released in same proportions that they are found in the plagioclase being weathered, namely of 0.62:0.38, if kaolinite is the weathering product. When Ca concentrations reach the point that smectite is stable, we would expect no further increase in Ca concentration, but Na should continue to increase. This is the path BD. Though the data show considerable scatter, and some springs are oversaturated with respect to smectite, the data generally support the conclusion that smectite is also a weathering product.

Garrels (1967) found that many springs in various other terranes also showed a similar cutoff in the kaolinite-smectite reaction quotient, suggesting formation of smectite is an important control on water chemistry. We should point out here that the controlling reaction need not be kaolinite to smectite. Direct weathering of plagioclase to smectite occurring when the solution becomes saturated with respect to smectite produces the same pattern. Also, the equilibrium constant for this reaction has not been directly measured. Indeed, the free energy of formation of smectite, which does not form crystals large enough to make thermodynamic measurements on, is deduced from this plot.

COWEETA BASIN, SOUTHERN APPALACHIANS

Velbel (1985a, 1985b) used a mass balance approach in his study of the Coweeta Basin to calculate rates of mineral weathering in a natural environment. The Coweeta Basin, an area of 1625 hectares located in southwestern-most South Carolina, had been subject of the a number of ecological studies and intensive hydrologic monitoring by the U. S. Forest Service and others for decades. Thus data on

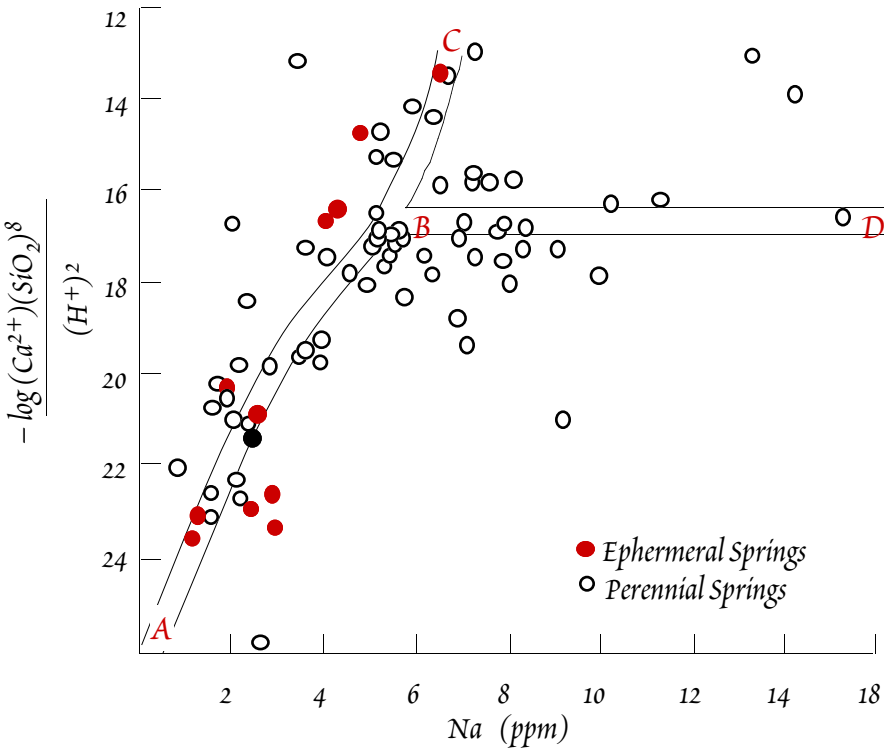

Figure 13.7. Reaction quotient for the Ca-beidellite—kaolinite reaction vs. sodium concentration. Data for the Sierra Nevada Springs is shown, as well as predicted evolution path for spring water during the weathering of plagioclase. From Garrels and McKenzie (1967).

biomass uptake and stream water compositions and fluxes were already available. There had been no anthropogenic activity in the area for at least 50 years before Velbel's work; disturbance before that was limited to controlled selection logging, so the biomass was close to steady-state. Annual rainfall is high, ranging from 170 cm at lower elevations (670 m) to 250 at higher elevations (up to 1600 m). Bedrock consists of a variety of metasediments and metavolcanics consisting of quartz, muscovite, biotite, plagioclase (oligoclase) and almandine garnet along with a variety of accessory minerals. This is overlain by soil averaging about 6 m in depth; 95% of this thickness is saprolite (C horizon).

Velbel's (1985a) found from petrographic, electron microprobe, and x-ray diffraction study that the primary weathering reactions were the breakdown of biotite, garnet, and feldspar; muscovite and quartz were not appreciably weathered and abundances of other minerals were too small to affect the mass balance. Biotite weathers initially to form hydrobiotite, a mixed-layer biotite-vermiculite. The primary lattice structure is preserved in this process, which involves loss of K (and some Mg), oxidation of Fe, and uptake of dissolved Fe and Al, and some Ca. The reaction may be written approximately as:

$$K(Mg_{1.2}Fe^{2+}_{1.3}Al_{0.5})(AlSi_3)O_{10}(OH)_2 + 0.2O_2 + 0.1H^+ + 0.3H_2O + 0.02Ca^{2+} + 0.3Al(OH)^+_{2(aq)} + 0.3Fe(OH)^+_{2(aq)}$$

$$\rightleftarrows K_{0.25}Ca_{0.02}(Mg_{1.1}Fe^{2+}_{0.5}Fe^{3+}_{1.1})(AlSi_3)O_{10}(OH)_2 \bullet 0.14Al_6(OH)_{15} + 0.75K^+ + 0.1Mg^{2+}$$

(some dissolved Na^+ is also consumed in this reaction, but we have ignored it for clarity). Upon further weathering, the hydrobiotite is transformed to vermiculite and/or "pedogenic chlorite".

Almandine garnet weathers congruently. Within the C horizon, local reprecipitation of the iron as goethite and some of the aluminum as gibbsite produces a protective surface layer on almandine and weathering reactions are limited by the rate of transport of reactants and products across the layer. In higher soil horizons, organic chelating agents remove the iron and aluminim and weathering is limited only by the rate of surface reactions.

Plagioclase weathers by selective attack at defects in the lattice. In early stages of weathering, components are removed in solution and reprecipitated elsewhere. The weathering reaction may be described as:

$$Ca_{0.25}Na_{0.75}(Al_{1.25}Si_{2.75})O_8 + 2.5H^+ + 5.5H_2O \rightleftarrows 0.25Ca^{2+} + 0.75Na^+ + 2.75H_4SiO_{4(aq)} + 1.25Al(OH)^+_{2(aq)}$$

In the second stage of weathering, precipitation of gibbsite and kaolinite occurs, in some cases close to the site of original dissolution, forming clay-mineral pseudomorphs of the original feldspar.

Table 13.7. Composition of Water from the Coweeta Watershed

	K	Na	Ca	Mg	pH
Soil	0.92	0.27	2.48	1.27	6.12
Well	0.60	1.08	1.12	0.65	5.10
Stream	0.59	1.08	1.06	0.64	6.64

From Velbel (1985b),

The concentrations of major cations in stream water, well water from the base of the saprolite (saprolite-bedrock interface), and soil water (sampled at 25 cm depth) are shown in Table 13.7. It is apparent from the Table that well water is nearly identical in composition to stream water. This indicates that stream water chemistry is determined entirely by reactions occurring as it percolates through the saprolite, with the exception that subsequent to leaving the subsurface, the water equilibrates with the atmosphere, resulting in a loss of CO_2 and increase in pH. On a plot of log (a_{K^+}/a_{H^+}) vs. log (a_{H2SiO4}), the composistion of stream waters plot in the kaolinite stability field,. Other aspects of stream chemistry indicate that both gibbsite and kaolinite form, consistent with the observation that both minerals occur as weathering products. Velbel's summary of the weathering profile is shown in Figure 13.8. In the upper part of the soil profile, rapid flushing keeps dissolved silica concentrations low so that kaolinite stability is not attained and aluminium released by plagioclase weathering precipitates as gibbsite, or is consumed in the production of vermiculite and chlorite from biotite. Deeper in the soil profile, water is in prolonged contact with rock and acquires enough aluminum and silica to reach kaolinite saturation. Because the bedrock is highly impermeable, most water is eventually shunted laterally downslope and does not penetrate the bedrock. What little water does penetrate forms smectite in voids and fractures. These reactions, however, have little effect on stream chemistry.

To calculate weathering rates, Velbel (1985a) used a system of simultaneous mass balance equations. For each element, c, the net flux of the element out of the watershed (steam output minus rain input) can be expressed as the sum of its production or consumption in each weathering reaction as well as by the biomass, i.e.:

$$\Delta m_c = \sum_i \alpha_i \beta_{c,i} \qquad 13.19$$

where Δm_c is the net flux of element c out of the watershed, $\beta_{c,i}$ is the stoichiometric coefficient of element c in reaction i, and α_i is the number of moles produced by weathering reaction i. Both β and Δm are known; the α's are the unknowns. For the elements K, Na, Ca, and Mg there are then 4 equations and 4 unknowns (net biomass uptake and the rates of plagioclase, biotite, and garnet weathering), allowing Velbel to simultaneously solve for the 4 α terms.

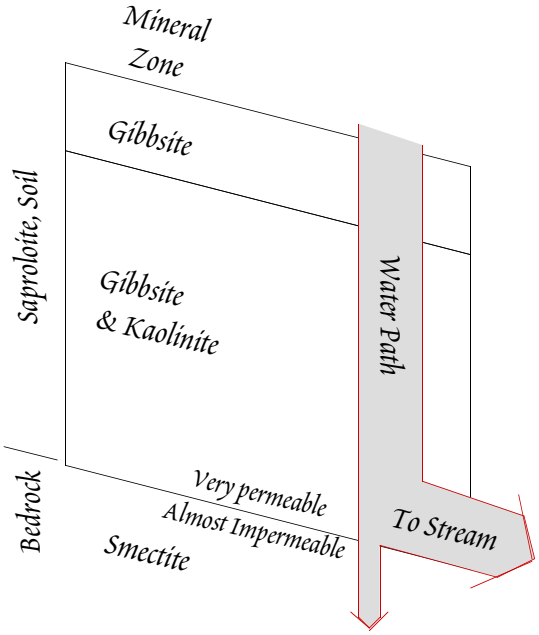

13.8. Schematic diagram of weathering profile and hydrology in the Coweeta Watershed. From Velbel (1985b).

Velbel calculated that 40,000 years were required to weather all the garnet, 140,000 years to react all the biotite, and 160,000 to weather all the plagioclase in the soil horizon. The calculated "saprolitization rate" was 3.8 to 15 cm/1000 yrs, the lower rate applying to complete destruction of primary minerals. This rate is nearly equal to the long term denudation, or erosion, rate (rate at which rock is removed from the surface) for the southern Appalachians. This agreement suggests the system is in

steady-state, i.e., weathering penetrates bedrock at same rate weathering products are removed by erosion, maintaining a constant thickness weathering profile. However, based on sediment export rates, the short-term denudation rates for the region were much slower, by as much as a factor of 20. This indicates that up to 96% of erosion occurs not by steady-state removal of soil, but by infrequent catestrophic events such as landslides and severe storms. This is entirely consistent with convention geologic views as well as other studies of erosion in the Southern Appalachians.

When normalized to estimated mineral surface areas, Velbel (1985a) found that calculated reactions rates of garnet and plagioclase were one to two orders of magnitude slower than measured laboratory rates. Drever and Clow (1995) point out that more recent laboratory experiments have produced lower dissolution rates: the discrpancy for plagioclase is a factor of two, that for biotite a factor of 8, and that for garnet a factor of 3.

It appears to be generally the case that weathering rates in nature are significantly slower than laboratory-determined rates (White, 1995; Drever and Clow, 1995). Velbel (1985a) suggested the difficulty in estimates of mineral surface area in natural systems as one possible cause of the discrepancy. Drever and Clow (1995) discuss several others possibililites, including aging and formation of protective surface layers on natural surfaces, the possible inhibitory effect of dissolved Al, and local approach to equilibrium in natural systems, which reduces the reaction affinity (i.e., ΔG, see Chapter 5) and slows the rate. In reviewing data from a number of studies, Velbel (1993) found that while laboratory rates are inevitably faster, the *ratio of rates* of dissolution of minerals determined from field and laboratory studies are similar. For example, the ratio of dissolution rate for olivine and plagioclase in the Filson Creek Watershed in Minnesota was 22, while the ratio of laboratory cation release rates from these minerals is 25. Velbel (1993) argued this implies that a physical, rather than chemical, factor is the cause of the discrepancy. He suggested the discrepancy arises because, in natural systems, water flow is heterogeneous and not all mineral surfaces are in contact with pore fluid and participate in reactions.

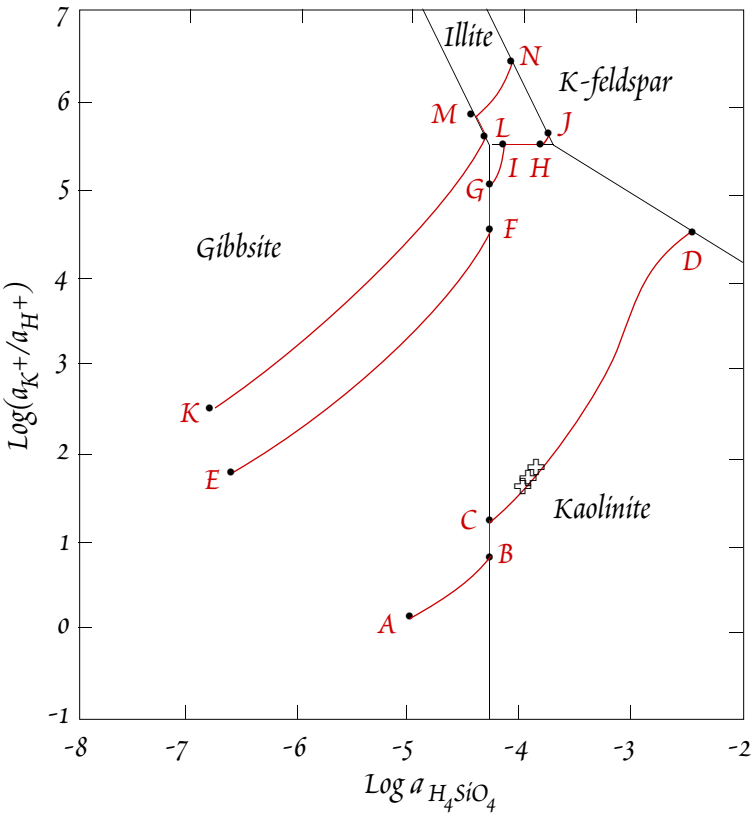

Figure 13.9. Stability diagram for the system K, OH, and H_2SiO_4 showing the solution path as weathering proceeds. (Illite is a clay mineral that is compositionally and structurally similar to the muscovite, $KAl_3Si_3O_{10}(OH)_2$, which most commonly forms in metamorphic rocks. Illite, however, is compositionally and structurally more variable. In particular, Si often substitutes for some Al and it has a deficit of K. In this analysis, we assume that illite is compositionally identical to muscovite.) Crosses show measured compositions of Coweeta stream water (Velbel, 1985b). Rainwater is presumably much more dilute, for example, the composition marked by point A. As weathering proceeds, the composition proceeds toward point C. Paths E-J and K-M are hypothetical paths of other possible solutions. See text for discussion.

CHAPTER 13: WEATHERING, SOILS, AND STREAM CHEMISTRY

Thermodynamic and Kinetic Assessment of Stream Compositions

As we found in the discussion of the Sierra Nevada spring water data, thermodynamics can provide insights as to what reactions are occurring in the weathering process. Let's consider the thermodynamics and kinetics of weathering in more detail, using the Coweeta study as an example. Figure 13.9 shows the stability diagram for the system K_2O-Al_2O_3-SiO_2-H_2O with the expected paths a solution would take in weathering of K-feldspar. Stream composition data from the Coweeta Watershed (Velbel, 1985b) are plotted on the diagram as crosses. The data plot within the kaolinite stability field, consistent with Velbel's observation that kaolinite is forming within the saprolite. The rainwater, however, is presumably much more dilute. Let's arbitrarily assume it plots at point A in Figure 13.9. This point plots within the gibbsite stability field. Thus from thermodynamics, we expect the initial weathering of feldspar will produce gibbsite. The reaction (considering only the K-component in the solid solution) is:

$$KAlSi_3O_8 + 7H_2O + H^+ \rightleftarrows K^+ + 3H_4SiO_{4(aq)} + Al(OH)_{3(s)} \qquad 13.20$$

This reaction produces dissolved K^+ and H_2SiO_4 and consumes H^+, so the composition of the water will evolve up and to the right toward point B on Figure 13.9 (the exact path depends on solution alkalinity because species such as H_2CO_3 can dissociate to partially replace the H^+ consumed in reaction 13.20).

When point B is reached, both kaolinite and gibbsite are stable, and any additional H_4SiO_4 produced by weathering of feldspar reacts with gibbsite to produce kaolinite:

$$KAlSi_3O_8 + 3Al(OH)_{3(s)} + H_4SiO_{4(aq)} + H^+ \rightleftarrows K^+ + 2Al_2Si_2O_5(OH)_4 + 3H_2O \qquad 13.21$$

The path is thus vertical along B–C until all gibbsite is consumed. Once it is consumed, further weathering produces kaolinite and dissolved K and H_2SiO_4 by the reaction:

$$KAlSi_3O_8 + 3H_2O \rightleftarrows K^+ + 2H_4SiO_{4(aq)} + \frac{1}{2}Al_2Si_2O_5(OH)_4 \qquad 13.22$$

The path (C–D) is steeper because less H_2SiO_4 is produced in weathering to kaolinite than to gibbsite. Eventually, the K^+ and H_2SiO_4 concentrations reach the point (D) where feldspar is stable, at which point no further weathering occurs because the solution is in equilibrium with K-feldspar.

Depending on the initial solution composition, other reaction paths are also possible. For example, a solution starting a point E in the gibbsite field would initially evolve in a similar manner to one starting a point A: producing first gibbsite then kaolinite. However, the solution starting a point E would eventually reach the illite stability field at point H. At this point, kaolinite is converted to illite through the reaction:

$$KAlSi_3O_8 + Al_2Si_2O_5(OH)_4 + 3H_2O \rightleftarrows KAl_3Si_3O_{10}(OH)_2 + 2H_4SiO_{4(aq)} \qquad 13.23$$

The K/H ratio is unaffected in this reaction, but the H_2SiO_4 concentration continues to increase. Once all kaolinite is consumed, further weathering of K-feldspar produces additional illite and the concentrations of H^+ decreases and K^+ and H_2SiO_4 increase again in the reaction:

$$3KAlSi_3O_8 + 12H_2O + 2H^+ \rightleftarrows 2K^+ + KAl_3Si_3O_{10}(OH)_2 + 6H_4SiO_{4(aq)} \qquad 13.24$$

This continues until the stability field of K-feldspar is reached. Yet other paths, such as K-N, may miss the kaolinite stability fields altogether.

This purely thermodynamic analysis does not predict the phases actually found in the weathering profile by Velbel (Figure 13.8), as both kaolinite and gibbsite occur together, while the water composition plots well within the kaolinite-only stability field. The problem arises because we have ignored kinetics. In essence, we have assumed that the dissolution of K-feldspar is slow, but that the solution quickly comes to equilibrium with secondary minerals such as gibbsite and kaolinite. Lasaga et al. (1994) have pointed out that such an assumption is naive. Let's consider the progress of the reaction along path A´-F´ from a kinetic perspective, but we follow the reaction with a reaction progress variable, ξ, which we define as the number of moles of feldspar consumed. Figure 13.10 is a reaction progess diagram showing the number of moles of secondary mineral produced as a function of ξ, under the assumption that equilibrium between solution and secondary minerals is fast. Gibbsite ini-

tially increases, then begins to decrease just as the stability boundary is reached as kaolinite begins to appear. There is a only limited region where both gibbsite and kaolinite are present (corresponding to path B-C on Figure 13.9). Once the boundary is past, only kaolinite is present.

Now let's assume that reaction rates are not infinitely fast, but that the rate of each reaction, *i*, depends on the extent of disequilibrium and can be described by the equation:

$$\Re_i = k_i \frac{\Delta G_i}{RT} \qquad 13.25$$

where $\Re$ is the reaction rate, *k* is the rate constant that includes a mineral surface area per mass term, and ΔG is the affinity of the reaction. This would be the case if each reaction behaved as an elementary one (compare equation 5.78). We further assume that the value of *k* is 10 times as large for the precipitation of gibbsite and kaolinte as for feldpar dissolution. The activity-activity and reaction progress diagrams computed by Lasaga et al. (1994) under these assumptions are shown in Figure 13.11. The activity-activity diagram is similar to that in Figure 13.9, although there is almost no vertical path along the gibbsite-kaolinite boundary. The reaction progress diagram, however, is quite different. We see that gibbsite and kaolinite now coexist over a wide region. This is a simple consequence of assuming finite rates for the precipitation reactions. Thus it is not surprsing that Velbel (1985a,b) found that gibbsite and kaolinite coexisted in the weathering profile even though the stream compositions plot within the kaolinite-only field.

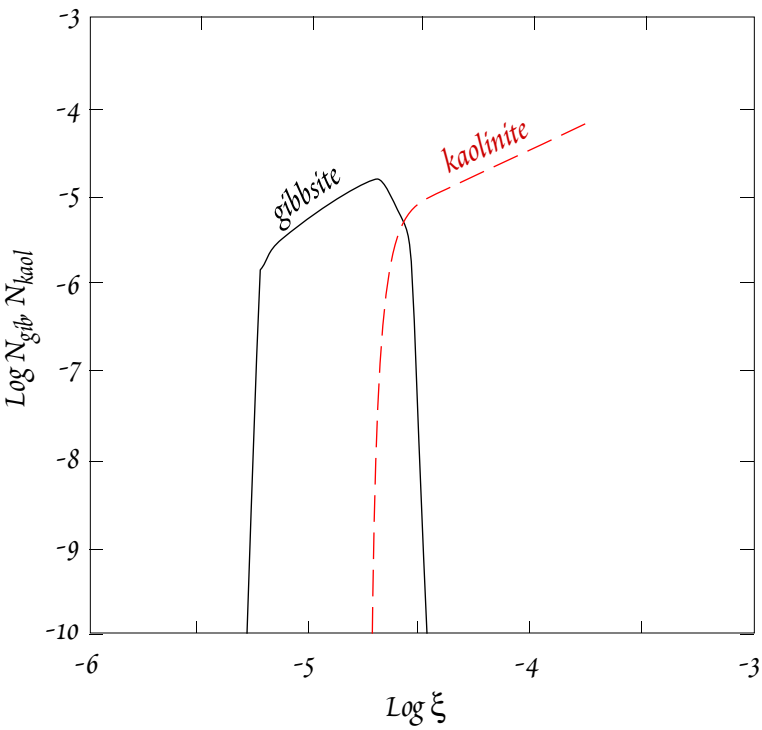

Figure13.10. Reaction progress diagram showing the number of moles of gibbsite and kaolinite produced as a function of ξ, the number of moles of feldspar consumed. This is the equilibrium case assuming infinitely fast equilibrium between the solution, gibbsite, and kaolinite. After Lasaga et al. (1994).

FACTORS CONTROLLING WEATHERING RATES

As we stated at the outset of this section, understanding the controls on weathering rates is of great interest to geochemists, primarily because of the role weathering plays as a sink for CO_2. Let's now consider the factors that control weathering rates. Lasaga et al. (1994) have proposed the following general form for the net rate law for weathering reactions:

$$\Re = A_{min} k_0 e^{-E_A/RT} a_{H^+}^n \prod_i a_i^{m_i} f(\Delta G_r) \qquad 13.26$$

where A_{min} is the mineral surface area, $ke^{-E_A/RT}$ expresses the usual dependence of the rate on temperature and activation energy (E_A), a_{H^+} expresses the dependence on pH to some power *n*, the terms $a_i^{m_i}$ represent possible catalytic or inhibitory effects of other ions, and $f(\Delta G_r)$ expresses the dependence of the reaction rate on the extent of dissequilibrium. As Lasaga et al. (1994) and the preceeding disucssion emphasize, any analysis of weathering rates must take account of the rates of formation of secondary minerals as well as the dissolution of primary ones. There is, however, less data on the former than the latter. This equation, which can be applied to both, provides a useful point of depar-

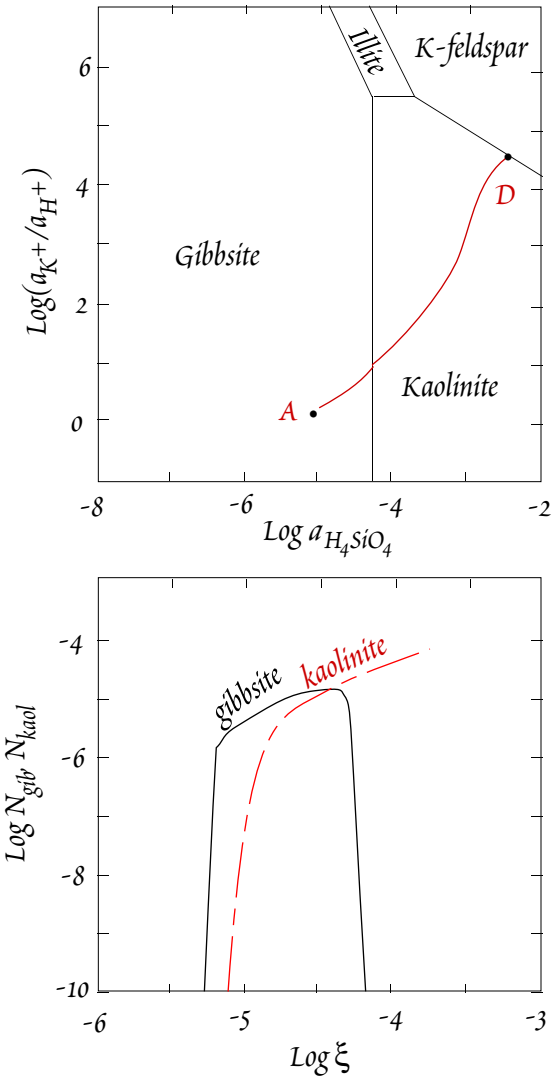

Figure 13.11. Stability and reaction progress diagrams computed assuming the rate constants for precipitation of gibbsite and kaolinite are only 10 times faster than that for the dissolution of feldspar. After Lasaga et al. (1994).

ture for our discusssion. Let's consider each of these terms in the natural, rather than laboratory, context.

The mineral surface area, or more accurately, the area of mineral surface in contact with reactive solution (ground, soil water), enters the equation as a simple linear term: the greater the surface area, the greater the reaction rate. Two factors in particular will control surface area: (1) rainfall and (2) the rate of physical weathering and erosion.

Where rainfall is insufficient to continually wet all grain surfaces, the rate of chemical weathering will be lower. Thus in arid regions, chemical weathering is slow. In some cases, this also results in low erosion rates. In others, where high rates of erosion result from high relief, glaciation, or some other factor, much of the material being removed will be fresh rock rather than weathering products. The relationship between precipitation and weathering is not simple, however. Bluth and Kump (1994) examined chemical weathering rates (using concentrations of bicarbonate and SiO_2 in streams as proxies for these rates) and found that the fluxes of SiO_2 and bicarbonate in streams from a given region remain constant over a large range of runoff, indicating that weathering rates increase with increasing precipitation. But bicarbonate and SiO_2 concentrations level off and even drop when runoff exceed 100 cm/yr, indicating, that additional precipitation is acting to merely dilute weathering products rather than increase weathering rates.

Rates of chemical weathering can also be slow even in humid tropical areas if the rate of erosion is sufficiently slow to allow thick soils to develop. This results is what Stallard and Edmond (1983) called a "transport-limited" regime, where thick lateritic soil (up to 100 m) insulates the underlying bedrock from chemical attack. Edmond et al. (1995) make the point that such tranport-limted regimes can occur even in areas of high elevation, such a the Guiana Shield in South America: "elevation per se is not the determing variable, but rather the mechanism by which it is produced." In tectonically active areas, such as the Andes, faulting generates high relief and exposes fresh rock to chemical weathering. Thus Edmond et al. emphasize the importance of tectonics in controlling global chemical weathering rates and, ultimately, atmospheric CO_2 levels. On the other hand, White and Blum (1995) found no correlation between chemical fluxes and relief, and argued that physical erosion rates do not have a critical influence of chemical weathering rates. However, the data they used came almost exclusively from North America and Europe, and thus did not include the tropical regions that were of primary interest to Edmond et al. (1995).

The $ke^{-E_A/RT}$ term in equation 13.26 expresses the usual Arrhenius exponential temperature dependence of reaction rates. We thus expect weathering rates to be higher in warm climates than in cold

ones, and this is indeed observed. The exact degree of temperature dependence will in turn depend on the activation energy. Various studies of the dependence of weathering rates on climate suggest the activation energy for chemical weathering is in the range of 40 to 80 kJ/mol (Lasaga et al., 1994; White and Blum, 1995). This is consistent with the average of activation energies of weathering reactions determined in laboratory studies (e.g., Table 5.4). This activation energy means that in increase in temperature of 8°C would result in a doubling of the weathering rate if all other factors remain constant.

Values of k and E_A vary from mineral to mineral (Table 5.4), hence weathering rates also depend on rock type. By examining stream composition in relation to rock type, Meybeck (1987) concluded that compared to granite, gneiss, and mica schist, gabbros and sandstones weathered 1.3 times as fast, volcanic rocks 1.5 times as fast, shales 2.5 times, serpentinites, marbles, and amphibolites 5 times, carbonates 12 times, gypsum 40 times, and rock salt 80 times as fast. These relative weathering rates are in at least qualitative agreement with rates predicted from laboratory studies of reaction rates (compare Table 5.3).

Numerous laboratory studies have found that the rates of weathering reactions depend on pH, but this dependence can be complex. In general, rates increase with decreasing pH in the acid range and increase with pH in the basic range. In some cases, rates appear to be independent of pH in the nuetral range. For example, Chow and Wollast (1985) found that the albite dissolution showed a dependence of the form a_{H^+} below pH 7 and a_{H^+} above it (see Figure 5.33). Though the data on ferromagesian silicates (such as pyroxenes and amphiboles) is less clear, it appears that the pH dependence is grossly similar, at least in the acid range, to that of feldspars (Brantley and Chen, 1995). pH of weathering solutions will depend primarily on three factors: dissolved CO_2, the presence of organic acids, and the extent of weathering. Biological activity in the soil increases dissolved CO_2 and decreases pH. At the same time, it releases organic acids that also decrease pH. On the other hand, weathering reactions consume H^+. Hence the pH of ground and soil water will progressively decrease as it reacts with rock. The presence of specific ions in solution may also affect reaction rates. For example, Chou and Wollast (1985) argued that dissolved Al inhibits feldspar dissolution, though this remains controverial. Organic acids may also have an effect on weathering rates beyond merely decreasing pH, because such acids can form surface complexes that directly promote weathering.

The final term in equation 13.26 expresses the expectation that reaction rates will decrease as equilibrium is approached. If the overall reaction rate is controlled by a single rate-limiting elementary reaction, we would expect this dependence to have the form predicted by transition state theory (see Chapter 5). However, Lasaga et al. (1994) point out that critical role played by crystal defects in weathering reaction leads to more a complex dependence of reaction rates on ΔG. The extent of disequilibrium will depend mainly on the rate at which water percolates through the soil. At high rates of flow, ΔG is large (i.e., equilibrium is not approached) and reaction rates are high. At lower flow rates, solution and rock more closely approach equilibrium and reaction rates slow. The dependence on ΔG helps explain the complex dependence of concentration on runoff observed by Bluth and Kump (1994).

The Effect of Plants on Weathering Rates

The biota clearly has an impact on chemical weathering, and for the most part, the effect of the biota is to increase weathering rates. Plants, and the soil microbes that survive on their detritus, increase soil P_{CO_2} and thereby decrease soil pH through respiration. They take up a variety of nutrients from the soil solution, and thus increase the disequilibrium between primary minerals and the soil solution. The decomposition products include organic acids, which also reduce soil pH. Plants also contribute to the physical disintigration of bedrock and by helping to form and retain a soil, keep rock in contact with water, which is essential for weathering reactions. Furthermore, transpiration returns water to the atmosphere, and hence increases rainfall. However, just how much terrestrial life has accelerated weathering is a matter of debate. Schwartzman and Volk (1989), for example, concluded that the existence of land plants has increased weathering rates by 2 to 3 orders of magnitude. Drever

(1994), however, argues that the direct chemical effect of land plants on weathering rates is probably no more than a factor of 2, and the overall effect is less than an order of magnitude.

Drever (1994) notes that the rates of many weathering reactions are independent of pH in the pH range of 4.5 to 8 (he acknowledges that weathering rates of many ferromagnesian silicates, such as pyroxenes and amphiboles, do increase with decreasing pH in this range). Most soil solutions have pH above 4.5, so pH decreases due to the biota have only a small effect on weathering rate. He also argues that while there is evidence that organic acids, such as oxalic acid, accelerate weathering reactions, the effect is typically only a factor of 2 at concentrations in the mM range. In nature, the organic acid concentrations are much lower and the overall effect of organic acids is likely to be much smaller. Although significant amounts of nutrients are stored in the biomass, mature ecosystems tend to be in steady state where the net uptake of nutrients is 0. Drever (1994) also points out that the effect of plants will be different depending on whether weathering is limited by rates of weathering reactions (weathering-limited) or by the tranport of weathering products. The Alps, where physical weathering and tranport of weathering products is rapid, are a good example of the former. Here, plants should cause an increase in weathering through increasing the contact time between water rock, hence their effect is to increase chemical weathering rates. The Amazon Basin, where weathering rates are extremely low, is an example of the latter. The combination of subdued topography and dense vegetation limits the rate at which weathering products can be tranported, leading to the accumulation of extremely deep (100 m) soils. The thick soil cover isolates the bedrock from incoming precipitation. Thus the effect of plants in the tranport-limited environment is to reduce chemical weathering rates.

The Composition of Rivers

Rivers return rain to the oceans. Except in estuaries, where river and sea water mixes, we think of river water as "fresh water". However, as can be seen from Table 13.8, river water is by no means pure, having on average about 100 ppm dissolved substances. Most, but not all, dissolved substances in rivers are the products of weathering. Some were present in rain to begin with. These "cyclic salts" enter the atmosphere via water droplets produced by breaking waves in the ocean. Since this is a physical process, there is little associated chemical fractionation and hence these seawater-derived salts are present in rain in the same concentrations as in seawater. Rain can also dissolve aerosols from other sources, such as continent-derived dust, compounds transpired by trees, volcanic ash and

TABLE 13.8 AVERAGE COMPOSITION OF DISSOLVED AND SUSPENDED LOADS OF RIVERS

	Ave Upper Crust	Ave Rain	Ave River Dissolved Load		Percent Cyclic	Ave River Suspended Load	River Dissolved /Crust	Suspended/ Dissolved
	mg/g	mg/kg	mg/kg	μM/kg		mg/kg	x 10^4	
Na	28.9	0.9	3.9	169.6	51%	6.6	1.35	0.5909
Mg	13.3	0.15	3.4	139.9	10%	11	2.56	0.3091
Al	80.4	–	0.04	1.5	–	97.4	0.00	0.0004
SiO_2	660	–	7.9	131.5	–	267	0.26	0.0296
K	28	0.23	1.45	37.2	35%	19.6	0.52	0.0740
Ca	30	1	14.5	362.5	15%	26	4.83	0.5577
Fe	35	–	0.05	0. 9	–	50.7	0.01	0.0010
Cl	_	1.13	4.7	132.6	53%	–	–	–
SO_4	_	2.02	8.5	88.5	52%	–	–	–
HCO_3	_ –		53.8	882.0	–	–	–	–
Total	_	5.43	98.24	209.6		478.3		

Average rain is U. S. average from Berner and Berner (1996). Average upper crust from Table 11.4, average river dissolved and suspended loads from Meybeck (1988). Polluted rivers were excluded in the average.

gases, pollutants, etc., so that total ionic concentrations in rain are not always in the same proportion as in seawater. In addition to cyclic salts and solutes derived from weathering, rivers also contain a variety of organic compounds derived from biological activity, as well as suspended solids, including both organic matter and mineral grains derived from erosion.

The composition of river water vary widely from the average given in Table 13.8. As we might expect, the major cations are the alkalis and alkaline earths, reflecting their relatively high solubility. Dissolved silica (usually reported as SiO_2 although the dominate dissolved species is H_4SiO_4) is also among the major dissolved species in rivers, though nevertheless depleted compared to it concentration in the crust and in the suspended load. This contrasts with seawater, where biological utilization results in very low SiO_2 concentrations. Concentrations of elements such as Fe and Al are extremely low, as we might expect. In most rivers, Ca^{2+} is the dominant cation and HCO_3 is the dominant anion. This contrasts with rain and seawater, where Na^+ and Cl^- are the dominant ions and reflects the importance of carbonate rock weathering in controlling river composition, as we discuss below. Table 13.9 lists the compositions of a number of rivers, selected to illustrate the range observed. River water composition depends on a number of factors, which we discuss below.

Those elements present in high dissolved concentrations tend to be depleted in the suspended load compared to average upper continental crust, and visa versa. This reflects the weathered nature of the suspended load carried by rivers: the most liable elements have been leached from them before the particles enter the river.

Gibbs (1970) used a plot of $Na^+/(Na^+ + Ca^{2+})$ versus total dissolved solids (TDS) to divide rivers into 3 classes: precipitation-dominated, rock-dominated, and evaporation/crystallization-dominated (Figure 13.12). He reasoned that rainfall has low TDS and high $Na^+/(Na^+ + Ca^{2+})$ and concluded that dissolved solids in rivers with these characteristics were derived mainly from precipitation. Reactions between water and rock (weathering) increase TDS and generally lower $Na^+/(Na^+ + Ca^{2+})$, thus rivers with these properties contained water that had interacted more extensively with rock. Evaporation increases TDS, and because calite and gypsum eventually crystallize from water when evaporative concentration occurs, the $Na^+/(Na^+ + Ca^{2+})$ ratio increases. Thus he reasoned that water with high TDS and $Na^+/(Na^+ + Ca^{2+})$ had undergone evaporative concentration and fractional crystallization of calcite and/or gypsum. Many rivers in this category, such as the Colorado and Rio Grande, come from arid regions, where evaporation rates are high.

Stallard and Edmond (1981, 1983), however, analyzed the composition of both precipitation and river water in the Amazon Basin and found that cyclic salts (i.e., those present in rain) contributed

Table 13.9. Representative Compositions of Major Rivers

	Negro	L. Amazon	Niger	Changjiang (Yangtze)	Mississippi	Nile	Hwanghe (Yellow)	Colorado
Na	0.4	1.5	3.5	7.6	11.0	17	55.6	95.0
Mg	0.1	1.0	2.6	7.4	8.9	7	17.7	24.0
SiO_2	4.1	7.2	15.0	6.9	7.6	21	5.1	9.3
K	0.3	0.8	2.4	1.5	2.8	4	2.9	5.0
Ca	0.2	5.2	4.1	30.2	34.0	25	42.0	83.0
Cl	0.3	1.1	1.3	9.1	10.3	8	46.9	82.0
SO_4	0.2	1.7	1.0	11.5	25.5	9	71.7	270.0
HCO_3	0.7	20.0	36.0	120.0	116.0	134	182.0	135.0
Total	6.3	38.5	65.9	194.2	216.1	224.7	423.9	703.3
Alk (μeq)	30.7	361.6	575.2	1991.8	2161.1	2263.2	3232.7	2449.3
ΣZ^+ (μeq)	43.3	428.0	632.7	2487.9	2982.6	2667.8	6048.5	10383.9
$SiO_2/\Sigma Z^+$	1.58	0.28	0.39	0.05	0.04	0.13	0.01	0.01

Concentrations in mg/l. Negro and Lower Amazon data from Stallard (1980), Changjiang and Hwanghe data from Zhang et al. (1990), others from Meybeck (1979).

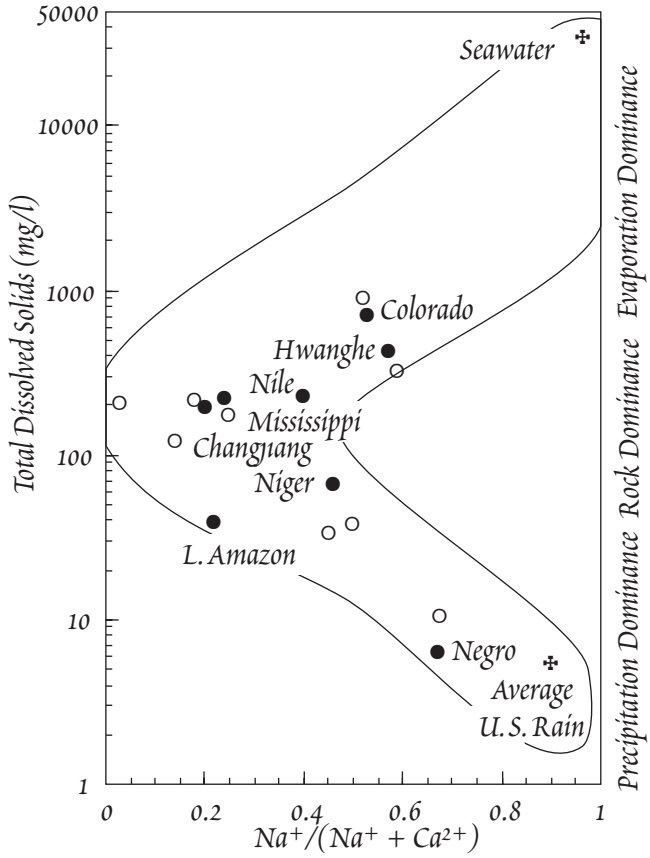

Figure 13.12. Plot of total dissolved solids vs. $Na^+/(Na^+ + Ca^{2+})$ used by Gibbs (1970) to define "precipitation-dominated", "rock-dominated", and "evaporation-dominated" river compositions. Solid symbols are the rivers in Table 13.9.

only a few percent of the total dissolved solids in rivers plotting within Gibb's "precipitation-dominated" field. Furthermore, these rivers had high ratios of SiO_2 to total cation charge ($SiO_2/\Sigma Z^+$), whereas rain has very low $SiO_2/\Sigma Z^+$. Stallard and Edmond (1983) proposed an alternative classification of rivers of the Amazon, based on ΣZ^+, and argued that *the principal factors controlling water chemistry are rock type and the intensity of weathering*. Berner and Berner (1996) showed that this classification can be extended to all rivers. The classification is as follows.

Transport-Limited Silicate Terranes. Stallard and Edmond's (1983) first category was rivers with $\Sigma Z^+ < 200$ μeg/l. They found that such rivers drain intensely weathered materials in a transport-limited regime (e.g., Rio Negro). Rivers in this category are enriched in SiO_2, Al, Fe, and organic anions and have a low pH. Perhaps the most significant feature of rivers in this category is their high ($SiO_2/\Sigma Z^+$). The $SiO_2/\Sigma Z^+$ of the average upper crust is 2.4; silicate sedimentary rocks, derived from rocks that have been partially weathered have a somewhat higher ratio (for example, the ratio in riverine suspended matter is 3.2). Taken to its extreme, weathering leaves a residue of Fe and Al oxides, quantitatively stripping the alkali and alkaline earth cations as well as silica. Thus the most intense weathering would produce water with $SiO_2/\Sigma Z^+$ of 2.4 or above, depending on the nature of the bedrock. Where weathering is somewhat less intense, leaving a kaolinite residue for example, the expected ratio would be closer to 1. Whereas in most rivers, the bicarbonate concentration approximately equals the total alkalinity, indicating carbonate species are the principal non-conservative ions, bicarbonate concentrations are much lower than alkalinity in rivers in this category. This is a result of high concentrations of organic anions, which account for much of the alkalinity total anion concentration.

Weathering-Limited Silicate Terranes. Stallard and Edmond (1983) proposed that rivers with ΣZ^+ between 200 and 450 μeq/l drained "weathering-limited siliceous terranes" (e.g., Congo, Amazon). In such regions the rate of erosion exceeds the rate of chemical weathering, and cations are leached from minerals in preference to SiO_2, leading to lower $SiO_2/\Sigma Z^+$ ratios of the water, while the availability of fresh rock results in higher ΣZ^+ and TDS than in transport-limited regimes. Rivers in this category have ($SiO_2/\Sigma Z^+$) of between 0.1 and 0.5.

Carbonate Terranes. Stallard and Edmond's third category was those rivers with ΣZ^+ between 450 and 3000 μeq/l. Such rivers have low $Na^+/(Na^+ + Ca^{2+})$ and high Ca, Mg, alkalinity, SO_4 (from oxidation of pyrite in reduced shales). Also, such rivers tend to have 1:1 ratios of Na to Cl and (Mg+Ca) to ($HCO_3 + SO_4$). These features indicate that these ions are derived from weathering of carbonates and evaporite minerals such as halite and gyspum. Rivers with these properties tend to drain areas

underlain by marine sediments containing carbonates, reduced shales, and minor evaporites. Most of the worlds major rivers fall in this category (Berner and Berner, 1996).

Evaporite Terranes. The fourth category of Stallard and Edmond was those rivers with $\Sigma Z^+ > 3000$ μeq/l. These rivers also tend to have 1:1 ratios of Na to Cl and (Mg+Ca) to (HCO_3 $+SO_4$). Such high ionic strength rivers drain terranes with abundant evaporites. Rivers in this and the third category have $SiO_2/\Sigma Z^+$ less than 0.1.

Stallard and Edmond (1983) used a ternary plot of carbonate alkalinity (HCO_3), SiO_2, and $Cl + SO_4$ (all in μeq/l) to illustrate the differences between these categories of rivers. A similar plot is shown in Figure 13.13, showing data from river compositions listed in Table 13.9.

Maybeck (1987) also emphasized the importance of rock type in controlling river dissolved load composition. He compared data from French rivers draining monolithic watersheds to data for global rivers. He found that "crystalline" (i.e., igneous and metamorphic) silicate rocks have only a minor influence on dissolved loads. Crystalline rocks account for 34% of the global surface rock outcrop, but only 12% of the global riverine dissolved load. In contrast, evaporites constitute only 1.25% of the outcrop, but 17% of the dissolved load. Carbonate rocks, which constitute 16% of the outcrop, account for half of the global riverine dissolved load. This is consistent with the observation that most major rivers fall in Stallard and Edmond's carbonate category, even through carbonate rocks are rarer than silicate ones. At a more fundamental level, it is the weathering rates of minerals the are important in controlling river chemistry: silicates release dissolved components slowly; carbonates and evaporites dissolve rapidly.

Although it is clear that rock type and weathering regime (transport-limted vs. weathering limited) are the most important factors controlling river chemistry, we should emphasize that both precipitation and evapotranspiration do play some role, albeit a lesser one. The concentration of cyclic salts in rain decrease with distance from the ocean. For exam-

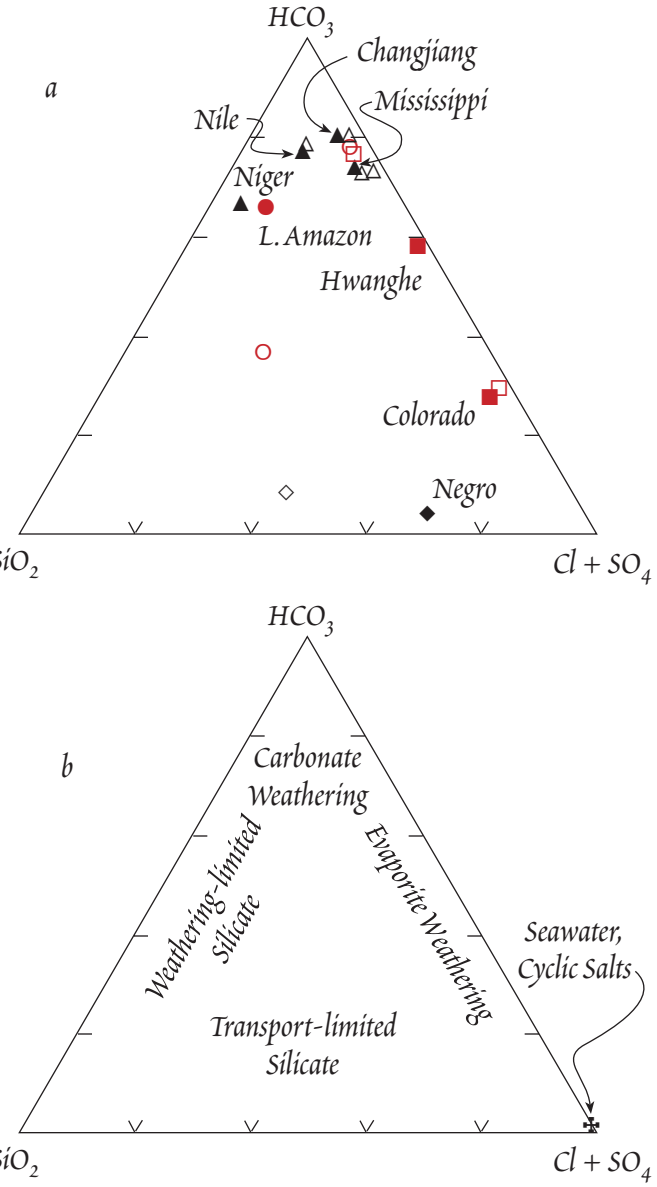

Figure 13.13. Ternary plot of SiO_2, $Cl + SO_4$, and HCO_3 (equivalent to carbonate alkalinity) used by Stallard and Edmond (1993) to illustrate how rock type and weathering intensity control river composition. (a) shows representative major rivers. Symbols are: diamonds: $\Sigma Z^+ < 200$ μeq, circles: $200 < \Sigma Z^+ < 450$ μeq, triangles: $450 < \Sigma Z^+ < 3000$ μeq, squares: $\Sigma Z^+ > 3000$ μeq. Filled symbols are rivers listed in Table 13.9. (b) shows where Stalland and Edmond's (1983) 4 categories plot.

ple, concentrations of Cl^- in rain in the Amazon Basin measured by Stallard and Edmond (1981) were as high as 200 mg/l near the mouth of the Amazon and as low as 2 mg/l at a station on the western edge of the basin 2800 km from the Atlantic coast. For this reason, coastal rivers in areas of high rainfall, such as the southeastern U.S., are the ones most likely to be truely precipitation-dominated (Berner and Berner, 1996). Evaporative concentration, and precipitation of calcite in soils, does indeed influence the composition of rivers draining arid regions such as the Colorado and Rio Grande. Agricultural use of water increases evaporation, as 2/3 or more of the water used in irrigation evaporates. Thus this activity serves to further increase the level of dissolved solids in such rivers.

CONTINENTAL SALINE WATERS

Saline waters result from evaporative concentration of fresh water. Table 12.14 lists the principal components in a number of brines from North America. As we might expect, there is a fair variation in concentrations, but a close inspection reveals something we might not expect: the relative concentrations of these elements also vary greatly. Some are carbonate brines, some are chlorine-rich brines. Some have high sulfate concentrations and some do not. Na^+ is always a major cation, but relative proportions of Ca^{2+} and Mg^{2+} vary greatly. What leads to this diversity in composition?

As is the case for rivers, the nature of the rock with which the source waters of saline lakes equilibrates is important in controlling concentrations. However, a number of other factors also play a role. Most important, perhaps, is the role of crystallization in magnifying relatively small differences in the composition of source waters. This is very much similar to the role played by crystallization in producing compositional diversity in igneous rocks. Let's consider what happens when dissolved solids in water are evaporatively concentrated.

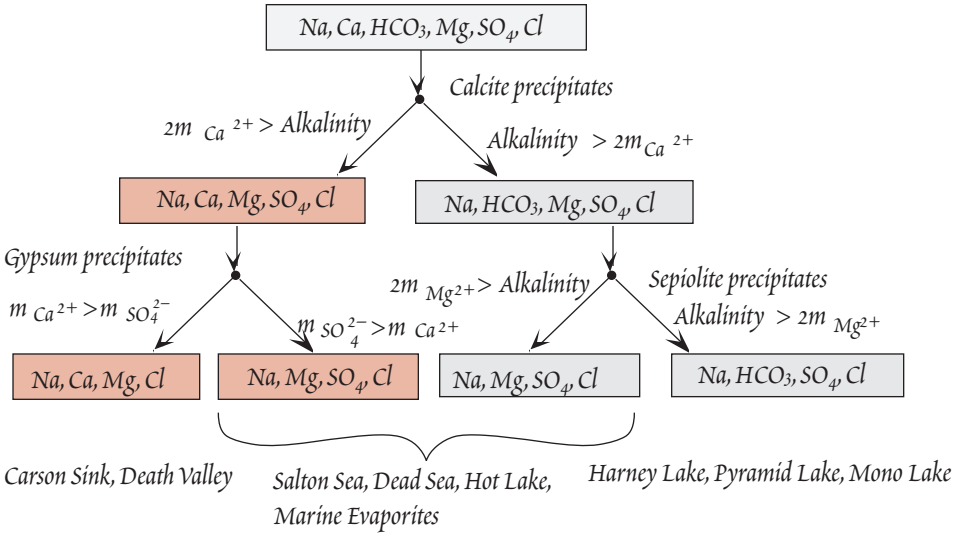

Figure 13.14. Chemical divides and evolutionary paths of evaporating natural waters. After Drever (1988).

In almost all natural waters, the first mineral to precipitate will be calcite. If the molar concentrations of Ca^{2+} and CO_3^{2-} are equal, the precipitation of calcite does not change the relative concentrations of these two ions. If, however, the concentration of CO_3 exceeds that of Ca, even by a small amount, then crystallization of calcite leads to an increase in the relative concentration of CO_3 and a decrease in the concentration of Ca. As long as evaporation continues, calcite will continue to crystallize and Ca concentrations will continue to decrease, and those of CO_3 to increase. This process leads to a Ca-poor, CO_3-rich brine. If the opposite is true, namely [Ca]>[CO_3], then Ca increases and CO_3 decreases, leading to a CO_3 poor brine. This illustrates the concept of *chemical divide*, which is shown in Figure 13.14. Depending on initial composition, an evaporating solution will come to forks in the compositional evolution paths that lead to very different compositions.

TABLE 13.10. NORTH AMERICAN SALINE LAKE BRINES

	Kamloops Lake No. 7, B.C.	Hot Lake, Wash.	Lenore Lake, Wash.	Harney Lake, Ore.	Alkali Valley, Ore.	Abert Lake, Ore.	Surprise Valley, Calif.	Great Salt Lake, Utah	Honey Lake, Calif.	Pyramid Lake, Nev.
SiO_2	—		22	31	542	645	36	48	55	1.4
Ca	tr	640	3	7	-	-	11	241	-	10
Mg	34,900	22,838	20	tr	-	-	31	7,200	-	113
Na	10,900	7,337	5,360	8,826	117,000	119,000	4,090	83,600	18,300	1,630
K		891	c	336	8,850	3,890	11	4,070	1,630	134
HCO_3	2,400	6,296	6,090	4,425	2,510	-	1,410	251	5,490	1,390
CO_3	-	-	3,020	d	91,400	60,300	644	-	8,020	-
SO_4	160,800	103,680	2,180	1,929	46,300	9,230	900	16,400	12,100	264
CI	200	1,688	1,360	6,804	45,700	115,000	4,110	140,000	9,680	1,960
Total	209,000	143,000	18,000	22,383	314,000	309,000	10,600	254,000	52,900	5,510
pH					10.1	9.8	9.2	7.4	9.7	

	Carson Sink, Nev.	Rhodes Marsh, Nev.	Mono Lake, Calif.	Saline Valley, Calif.	Owens Lake, Calif.	Death Valley Calif.	Searles Lake, Calif.	Soda Lake, Calif.	Danby Lake, Calif.	Salton Sea, Calif.
SiO_2	19	142	14	36	299	-		-	-	20.8
Ca	261	17	4.5	3.1	43	-	16	-	325	505
Mg	129	0.5	34	552	21	150		-	108	581
Na	56,800	3,680	21,500	103,000	81,398	109,318	110,000	114,213	137,580	6,249
K	3,240	102	1,170	4,830	3,462	4,043	26,000	tr	-	112
HCO_3	322	23	5,410	614	52,463	-	-	-	tr	232
CO_3	-	648	10,300	-	d		27,100	12,053	-	-
SO_4	786	2,590	7,380	22,900	21,220	44,356	46,000	52,026	13,397	4,139
CI	88,900	3,070	13,500	150,000	53,040	140,196	121,000	124,618	119,789	9,033
Total	152,000	10,400	56,600	282,360	213,700	299,500	336,000	305,137	271,200	20,900
pH	7.8	9.5	9.6	7.35						

Notes tr: trace. c: Reported Na represents Na + K. d: Reported HCO_3 represents $HCO_3 + CO_3$. From Eugster and Hardie (1978).

The first divide is, as we have seen, calcite. Depending on the path taken at that divide, the next divide is either precipitation of gypsum or precipitation of a Mg mineral, either dolomite or sepiolite ($Mg_4Si_6O_{15}(OH)_2 \cdot 6H_2O$, a mixed-layer, 2:1 clay). Gypsum precipitation leads to either a sulfate-depleted or calcium-depleted brine. Although dolomite is the Mg mineral predicted by thermodynamics to precipitate in Mg, CO_3 rich waters, dolomite reactions are so sluggish that sepiolite is actually more likely to precipitate. Both dolomite and sepiolite lead to either magnesium or carbonate depleted brines, because both reactions consume carbonate:

$$Mg^{2+} + 2HCO_3^- + 3H_4SiO_4 \rightleftarrows MgSi_3O_6(OH)_2 + 2CO_2 + 6H_2O \qquad 13.27$$

Note that most of the chloride, and often much of the sulfate and sodium in saline lakes is derived from rain. Sodium and chloride minerals precipitate only at extreme concentrations.

Several other factors play a role in determining the composition of saline waters. One is whether sulfate reduction occurs. The solubility of oxygen decreases with increasing salinity, so reducing conditions are more likely in saline than in fresh waters. Sulfate reduction obviously depletes sulfate (by converting it to insoluble sulfides), but it also increases carbonate alkalinity by production of carbonate by oxidation of organic matter. Another factor is ion exchange and absorption. Many saline lakes are fed by subsurface flow, providing the opportunity for ion exchange with clays and other minerals. This accounts for the low K concentrations of most saline waters. Finally, cyclic wetting and drying can lead to some interesting effects resulting from kinetics. In dry periods, evaporite minerals will precipitate subsurface. Rains in many dry areas come as occasional or rare cloud bursts and

may wet the soil long enough to dissolve highly soluble salts such as sodium chloride, but not long enough to achieve equilibrium with slightly soluble salts such as gypsum. This can lead to sulfate concentrations lower than that expected from evaporative concentration of rain water.

REFERENCES AND SUGGESTIONS FOR FURTHER READING

Berner, R. A., A. C. Lasaga, and R. M. Garrells. 1983. The carbonate-silicate geochemical cycle and its effect on atmopsheric carbon dioxide over the past 100 million years. *Amer. J. Sci.* 283: 641-683.

Berner, E. K. and R. A. Berner, 1996. Global Environment: Water, Air, and Geochemical Cycles, Upper Saddle River (NJ): Prentice Hall.

Berner, R. A. 1991. Atmospheric CO_2 levels over Phanerozoic time. *Science*. 249: 1382-1386.

Bluth, G. J. S. and L. R. Kump. 1994. Lithologic and climatological controls of river chemistry. *Geochim. Cosmochim. Acta*. 58: 2341-2360.

Brantley, S. L. and Y. Chen.1995. Chemical weathering rates of pyroxenes and amphiboles. in *Chemical Weathering Rates of Silicate Minerals, Reviews in Mineralogy 31*, ed. A. F. White and S. L. Brantley. 119-172. Washington: Min. Soc. Amer.

Brimhall, G. H. and W. E. Dietrich. 1987. Constitutive mass balance relations between chemical composition, volume, density, porposity, and strain in metasomatic hydrochemical systems: results on weathering and pedogenesis. *Geochim. Cosmochim. Acta*. 51: 567-588.

Brooks, R. R. 1972. *Geobotany and Biogeochemistry in Mineral Exploration*. New York: Harper and Row.

Chou, L. and R. Wollast. 1985. Steady-state kinetics and dissolution mechanisms of albite. *Amer. J. Sci.* 285: 965-993.

Drever, J. I. (ed.), 1985, *The Chemistry of Weathering*, Dordrecht: D. Reidel Publ. Co.

Drever, J. I., 1988. *The Geochemistry of Natural Waters,* Prentice Hall, Englewood Cliffs, 437 p.

Drever, J. I. 1994. The effect of land plants on weathering rates of silicate minerals. *Geochim. Cosmochim. Acta*. 58: 2325-2332.

Drever, J. I. and D. W. Clow. 1995. Weathering rates in catchments. in *Chemical Weathering Rates of Silicate Minerals, Reviews in Mineralogy 31*, ed. A. F. White and S. L. Brantley. 463-483. Washington: Min. Soc. Am.

Edmond, J. M., M. R. Palmer, C. I. Measures, B. Grant and R. F. Stalland. 1995. The fluvial geochemistry and denudation rate of the Guayana Shield in Venezuela, Columbia, and Brazil. *Geochim. Cosmochim. Acta*. 59: 3301-3326.

Eugster, H. P. and L. A. Hardie, 1978, Saline Lakes, in *Lakes—Chemistry, Geology, Physics*, A. Lerman (ed.), Springer-Verlag, New York, pp. 237-293.

Feth, J. H., C. E. Roberson and W. L. Polzer. 1964. Sources of mineral constituents in water from granitic rocks, Sierra Nevada, California and Nevada: *U. S. Geol. Surv. Water-Supply Pap. 1535*

Garrels, R. M. 1967. Genesis of some ground waters from igneous rocks. in *Researches in Geochemistry, 2* ed. P. H. Abelson. 405-420. New York: Wiley.

Garrels, R. M. and C. L. Christ. 1965. *Solutions, Minerals and Equilibria*. New York: Harper and Row.

Garrels, R. M. and R. T. Mackenzie. 1967. Origin of the chemical composition of some springs and lakes. *Equilibrium Concepts in Natural Water Systems, Am Chem. Soc. Adv. Chem. Ser.* 67: 222-242.

Gibbs, R. J. 1970. Mechanisms controlling world water chemistry. *Science*. 170: 1088.

Lasaga, A. C., J. M. Soler, G. J., T. E. Burch and K. L. Nagy. 1994. Chemical weathering rate laws and global geochemical cycles. *Geochim. Cosmochim. Acta*. 58: 2361-2386.

Martin, J.-M. and M. Meybeck. 1979. Elemental mass balance of material carried by major world rivers. *Mar. Chem.* 7: 173-206.

Meybeck, M. 1979. Concentration des eaux fluviales en éléments majeurs et apports en solution aux océans. *Rev. Géo. Dyn. Géogr. Phys.* 21: 215-246.

Meybeck, M. 1987. Global chemical weathering of surficial rocks estimated from river dissolved loads. *Am. J. Sci.* 287: 400-428.

Meybeck, M.1988. How to establish and use world budgets of riverine materials. in *Physical and Chemical Weathering in the Global Environment*, ed. A. Lerman and M. Meybeck. 247-272. Dordrecht: D. Riedel Publ.

Morel, F. M. M. and J. G. Hering. 1993. *Principles and Applications of Aquatic Chemistry*. New York: John Wiley and Sons.

Probst, A., E. Dambrine, D. Viville and B. Fritz. 1990. Influence of acid atmospheric inputs on surface water chemistry and mineral fluxes in a declining spruce stand within a small granitic catchment (Vosage Massif, France). *J. Hydrol.* 116: 101-124.

Richardson, S. M. and H. Y. McSween. 1988. *Geochemistry: Pathways and Processes*, New York: Prentice Hall.

Robbins, J. A. and E. Callender. 1965. Diagenesis of manganese in Lake Michigan sediments. *Am. J. Sci.* 275: 512-533.

Schlesinger, W. H. 1991. *Biogeochemistry*. San Diego: Academic Press.

Schwartzman, D. W. and T. Volk. 1989. Biotic enhancement of weathering and the habitability of the Earth. *Nature*. 340: 457-460.

Sposito, G. 1989. *The Chemistry of Soils*. New York: Oxford University Press.

Stallard, R. F. 1980. *Major Element Geochemistry of the Amazon River System*. PhD Dissert. Cambridge: M. I. T.

Stallard, R. F. 1985. River chemistry, geology, geomorphology, and soils in the Amazon and Oronoco Basins. in *The Chemistry of Weathering*, ed. J. I. Drever. 293. Dordrecht: D. Reidel Publ.

Stallard, R. F. and J. M. Edmond. 1981. Geochemistry of the Amazon 1. Precipitation chemistry and the marine contribution to the dissolved load at the time of peak discharge. *J. Geophys. Res.* 86: 9844-9858.

Stallard, R. F. and J. M. Edmond. 1983. Geochemistry of the Amazon 2. The influence of geology and weathering environment on the dissolved load. *J. Geophys. Res.* 88: 9671-9688.

Stallard, R. F. and J. M. Edmond. 1987. Geochemistry of the Amazon 3. Weathering chemistry and the limits to dissolved inputs. *J. Geophys. Res.* 92: 8293-8302.

Stumm, W. and J. J. Morgan. 1995. *Aquatic Chemistry*, New York: Wiley and Sons.

Velbel, M. A. 1985a. Geochemical mass balances and weathering rates in forested watersheds of the Southern Blue Ridge. *Am. J. Sci.* 285: 904-930.

Velbel, M. A. 1985b. Hydrogeochemical constraints on mass balances in forested watersheds of the Southern Appalachians. in *The Chemistry of Weathering*, ed. J. I. Drever. 231-247. Dordrecht: D. Reidel Publ. Co.

Velbel, M. A. 1993. Constancy of silicate-mineral weathering-rate ratios between natural and experimental weathering: implications for hydrologic control of differences in absolute rates. *Chem. Geol.* 105: 89-99.

White, A. F.1995. Chemical Weathering rates of silicate minerals in soils. in *Chemical Weathering Rates of Silicate Minerals, Reviews in Mineralogy 31*, ed. W. A. F. and S. L. Brantley. 407-461. Washington: Min. Soc. Am.

White, A. F. and A. E. Blum. 1995. Effects of climate on chemical weathering in watersheds. *Geochim. Cosmochim. Acta*. 59: 1729-1747.

White, A. F. and S. L. Brantley (ed.), 1995, *Chemical Weathering Rates in Silicate Minerals*, Washington: Mineral. Soc. Am.

Zhang, J. W., W. Huang, M. G. Lin and A. Zhon. 1990. Drainage basin weathering and majro element transport of two large Chinese rivers (Hwanghe and Changjiang). *J. Geophys. Res.* 95: 13277-13288.

PROBLEMS

1. The dissolution of *talc* may be described by the reaction:

$$Mg_3Si_4O_{10}(OH)_2 + 6H^+ + 4H_2O \rightleftarrows 3Mg^{2+} + 4H_4SiO_4 \qquad (1)$$

that of *brucite* as:

$$Mg(OH)_2 + 2H^+ + 4H_2O \rightleftarrows Mg^{2+} + 2H_2O \quad (2)$$

and that of *serpentine* as:

$$Mg_3Si_2O_5(OH)_4 + 6H^+ \rightleftarrows 3Mg^{2+} + 2H_4SiO_4 + H_2O \quad (3)$$

The solubility of quartz is 10^{-4}. The ΔG for these reactions (at 25° C) have been estimated as -114.09 kJ, -96.98 kJ, and -193.96 kJ respectively. On a plot of log $([Mg^{2+}]/[H^+]^2)$ vs. log $[H_4SiO_4]$ show the stability fields for talc, brucite, and serpentine.

2. For this question, assume that the dissolution rate of brucite shows the dependence on ΔG given in equation 6.48, that the value of k_i is 10^{-6} moles/sec, and a temperature of 25°C. If all other factors remain constant, how will the dissolution rate change as equilibrium between brucite and solution is approached? Make a plot showing the *relative* reaction rate as a function of log $([Mg^{2+}]/[H^+]^2)$.

3. The following is an analysis of the Congo River in Africa (units are mg/l).

pH	Ca^{2+}	Mg^{2+}	Na^+	K^+	Cl^-	SO_4	HCO_3	SiO_2	TDS
6.87	2.37	1.38	1.99	1.40	1.40	1.17	13.43	10.36	54

a. Calculate the *alkalinity* of this water. How does alkalinity compare to the bicarbonate concentration (*HINT:* be sure to use molar units in your comparison).
b. Based on the $Na^+/(Na^+ + Ca^{2+})$ ratio (mg/l) of this analysis, into which of Gibb's 3 categories would you play the Congo River?
c. Calculate ΣZ^+ (μeq/l). Into which of Stallard and Edmond's categories would this river fall?
d. Calculate the $\Sigma Z^+ / SiO_2$ (μeq/μM) ratio for this river. Do all calculations at 25°C.

4. Referring to Figure 6.22, would you expect the Congo River water of Problem 3 to be in equilibrium with gibbsite, kaolinite, muscovite, pyrophyllite, or K-feldspar?

5. Assuming a dissolved aluminum concentration of 0.05 mg/l in Congo River water, calculate the concentration of the various aluminum species at the pH given in problem 2 and the equilibrium constants in equations 6.68 through 6.71.

6. Use the analysis of Congo River water in Problem 3 for these questions.
a. What is the ionic strength of this solution?
b. Calculate the Debye-Hückel activity coefficients for this solution.
c. The bicarbonate concentration reported is actually total carbonate (ΣCO_2). Calculate the actual concentrations of each of the 3 carbonate species.
d. Calculate the buffer capacity of this water at the given pH and assuming all ions other than the carbonate species remain completely dissociated.

7. Calculate the *speciation* of the ions listed in the Congo River water analysis in Problem 3. Use the stability constants given in Example 6.7.